

Dear Prof. David Carlson,

All the coauthors greatly appreciate you for your positive comments on our revisions, as well as the kind decision “Publish subject to minor revisions (review by editor)”. Though minor revision is needed, we still have paid great attentions on each bullet pointed out by you, and also checked the manuscript carefully for the typos, missing co-authors and their affiliations, terminology, updates of data in tables, and updates of variables in equations accordingly. Additionally, all of the figures (Fig. 1-14) have been revised and updated to meet the standard for the publication.

As required by this Journal, the responses to the Referees/Editors should be structured in a clear and easy-to-follow sequence: (1) comments from Referees/Editors, (2) author's response, and (3) author's changes in manuscript. Therefore, we have responded to your comments in the following sequence: the original comments in **black**, our responses in **blue**, and our changes in manuscript in **red**.

**The details of the point-by-point replay and the corresponding revised manuscript are shown in the following section.**

We hope that the manuscript at this stage could be accepted for the publication, and we are looking forward to hearing from you soon.

Yours sincerely,

Dr. Ziqiang Ma; Prof. Yang Hong

Institute of Remote Sensing and Geographical Information System, School of Earth and Space Sciences, Peking University, Beijing, 100871, China

School of Civil Engineering and Environmental Science, University of Oklahoma, Norman, OK, 73019, United States

Emails: [ziqma@pku.edu.cn](mailto:ziqma@pku.edu.cn) ; [hongyang@ou.edu](mailto:hongyang@ou.edu)

## Point-by-point reply to the Topical Editor

Journal: ESSD

Title: AIMERG: a new Asian precipitation dataset (0.1°/half-hourly, 2000-2015) by calibrating GPM IMERG at daily scale using APHRODITE

Author(s): Ziqiang Ma et al.

MS No.: essd-2019-250

MS Type: Data description paper

**General Comments:** Very many improvements from original manuscript, thank you. Author team will need to work carefully with Copernicus publishing team during proof-reading, to correct remaining language-based inconsistencies. Authors may need to consider consulting with a native English technical writer.

**Authors Response:** All the coauthors greatly appreciate you for your positive comments on our revisions, as well as the kind decision “Publish subject to minor revisions (review by editor)”. Though minor revision is needed, we have paid great attentions on each bullet pointed out by you, and also checked the manuscript carefully for the typos, missing co-authors and their affiliations, terminology, updates of data in tables, and updates of variables in equations accordingly. **Additionally**, all of the figures (Fig. 1-14) have been revised and updated to meet the standard for the publication.

In terms of the remaining **language-based issues**, we will carefully collaborate with Copernicus publishing team during the proof-reading stage, and also would like to consult the **professional English language editing service** (<http://www.sciencemanager.com/>), who has helped us improving several Manuscripts for some other big journals, such as *Remote Sensing of Environment*.

-----

Below, the original comments are in **black**, our responses are in **blue**, and our changes in manuscript are in **red**.

**Point 1:**

**Editor’ Comments:** Line 185: "five datasets used in this study" but Table 1 lists only 4? The rain gauge from hydrological network seem missing? Mentioned again as an independent evaluation data set at lines 373, 374, etc?

**Authors Response:** Originally, we have list the “Point-based rain gauge data from meteorological stations” and “Point-based rain gauge data from hydrological stations” together as “Point-based rain gauge data”. However, it is really not clear for the readers. We have list all the five datasets separately in the Table 1.

**Author's changes in manuscript:** We have list all the five datasets accordingly in Table 1, in lines from 191 to 193, as follows:

**Table 1.** List of satellite-based, gauge-based, and satellite-gauge combination precipitation products used in this study.

Short name	Full name	Spatial and temporal sampling	Time period	References
IMERG	Integrated Multi-satellitE Retrievals for Global Precipitation Measurement	0.1°/half-hourly	2000-2015	Huffman et al. (2019b) <a href="https://pmm.nasa.gov/data-access/downloads/gpm">https://pmm.nasa.gov/data-access/downloads/gpm</a> (last access: 17 January 2020)
APHRODITE	Asian Precipitation Highly Resolved Observational Data Integration Towards Evaluation of Water Resources	0.25°/daily	1951-2015	Yatagai et al. (2012) <a href="http://aphrodite.st.hirosaki-u.ac.jp/download/">http://aphrodite.st.hirosaki-u.ac.jp/download/</a> (last access: 17 January 2020)
CMPA	China Merged Precipitation Analysis	0.1°/hourly	2008-2015	Shen et al. (2014) <a href="http://data.cma.cn">http://data.cma.cn</a> (last access: 17 January 2020)
	Point-based rain gauge data from meteorological stations	hourly	2015	Shen et al. (2010) <a href="http://data.cma.cn">http://data.cma.cn</a> (last access: 17 January 2020)
	Point-based rain gauge data from hydrological stations	hourly	2010-2015	Shen et al. (2010) <a href="http://data.cma.cn">http://data.cma.cn</a> (last access: 17 January 2020)

**Point 2:**

**Editor’ Comments:** Line. 242 and Table 2: Term MAE in text does not (but should) match term ME in Table 2?

**Authors Response:** After careful examinations, we find that we have made mistakes only in the descriptions in the Table 2. And we have replaced ME with MAE, as well as the expressions in the corresponding Equation, in Table 2.

**Author's changes in manuscript:** we have replaced ME with MAE, as well as the expressions in the corresponding Equation, in the Table 2, in line 252.

**Table 2** Formulas and perfect values of the evaluation metrics used in this study.

Statistic metrics	Equation	Perfect value	Value ranges
Correlation Coefficient (CC)	$CC = \frac{\frac{1}{N} \sum_{n=1}^N (S_n - \bar{S})(G_n - \bar{G})}{\sigma_S \sigma_G}$	1	[-1, 1]
Mean Absolute Error (MAE)	$MAE = \frac{1}{N} \sum_{n=1}^N ( S_n - G_n )$	0	(0, +∞)
Relative Bias (BIAS)	$BIAS = \frac{\sum_{n=1}^N (S_n - G_n)}{\sum_{i=1}^n G_n} \times 100\%$	0	(-∞, +)
Root Mean Square Error (RMSE)	$RMSE = \sqrt{\frac{1}{N} \sum_{n=1}^N (S_n - G_n)^2}$	0	[0, +∞)
Probability of Detection (POD)	$POD = \frac{n_{11}}{n_{11} + n_{01}}$	1	[0, 1]
False Alarm Ratio (FAR)	$FAR = \frac{n_{10}}{n_{11} + n_{10}}$	0	[0, 1]
Critical Success Index (CSI)	$CSI = \frac{n_{11}}{n_{11} + n_{10} + n_{01}}$	1	[0, 1]

**Point 3:**

**Editor' Comments:** Line 269, Figure 2: Units in this figure? mm/day? mm/month? mm/year?

**Authors Response:** The units in Figure 2 are all mm/year. To make it more clearly, we have added the units in Figure 2.

**Author's changes in manuscript:** we have added the units in Figure 2, in line 273. And the revised Figure 2 is shown as follows:



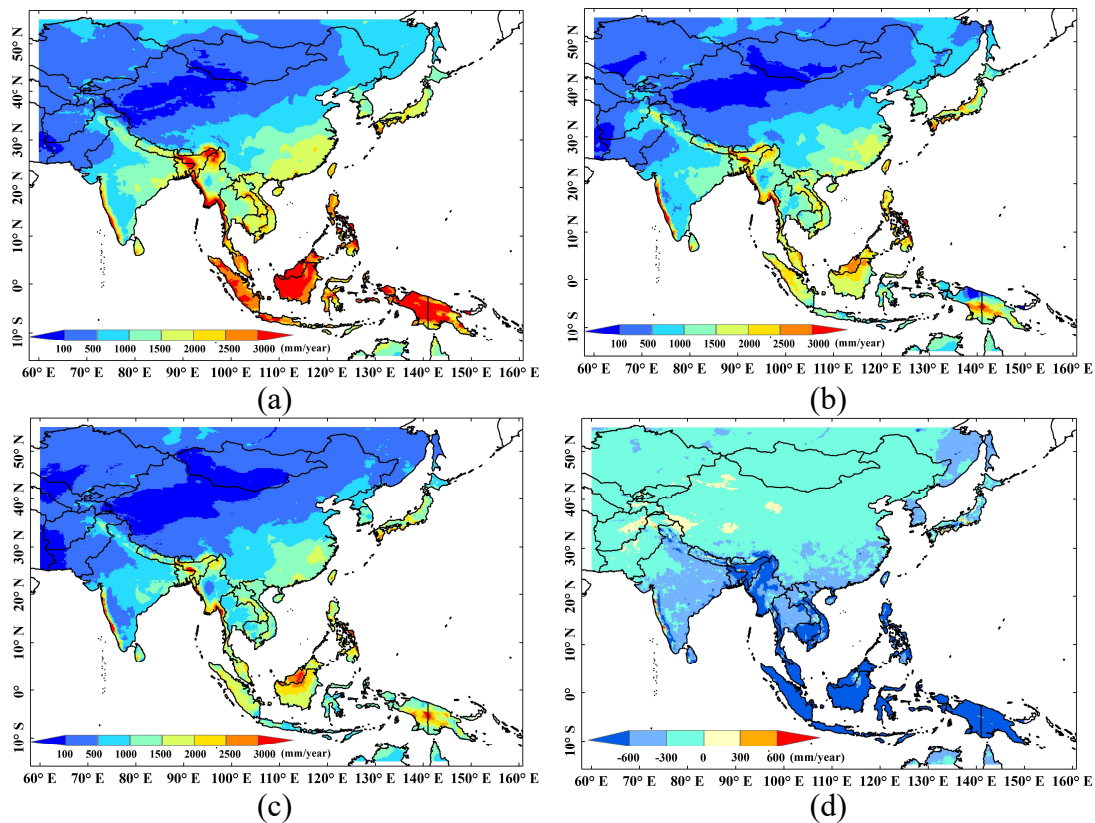


Figure 2. Spatial patterns of Asian mean annual gridded precipitation products of (a) IMERG, 0.1°, (b) APHRODITE, 0.25°, and (c) AIMERG, 0.1°, and (d) AIMERG-IMERG, 0.1°, respectively, during the period of 2001-2015.

**Point 4:**

**Editor' Comments:** Lines 264-266 - "Though AIMERG is smaller than IMERG over most regions, there are still some areas where the volumes of AIMERG are larger than those of IMERG, e.g., in western Tibetan Plateau, Middle East, and along the western coast of India". Figure 2d does not show this pattern?

**Authors Response:** From the legend in Figure 2d, we really find that the volumes of AIMERG are larger than those of IMERG, e.g., in western Tibetan Plateau, where the color is in pale yellow. To make it more clearly, we have changed the this sentence "Though AIMERG is smaller than IMERG over most regions, there are still some areas where the volumes of AIMERG are larger than those of IMERG, e.g., in western Tibetan Plateau, Middle East, and along the western coast of India" into "Though AIMERG is smaller than IMERG over most regions, there are still some areas where the volumes of AIMERG are larger than those of IMERG, e.g., in western Tibetan Plateau".

**Author's changes in manuscript:** The sentence "..., there are still some areas where the volumes of AIMERG are larger than those of IMERG, e.g., in western Tibetan Plateau, Middle East, and along the western coast of India" into "..., there are still some areas where the volumes of AIMERG are larger than those of IMERG, e.g., in western Tibetan Plateau" in line 269.

**Point 5:**

**Editor' Comments:** Figure 2: confusing to have background ocean (= bathymetry?) included in this and other figures. Better to mask the ocean with no or white-only color? Or solid color as in Figure 11?

**Authors Response:** Very good suggestion, to make it more clearly, we have removed the background ocean with no color. Additionally, we have updated all of the Figures, Fig. 1-14, and provided the corresponding figures according to the standard for publication, as required by "File submission for production of final revised paper".

**Author's changes in manuscript:** we have removed the background ocean with no color in Figure 2, 3, 9, 11, 13. And for all of these revised figures, please see them in the following revised manuscript with changes highlighted.

**Point 6:**

**Editor' Comments:** Line 395, Figure 10 especially hourly insets remains hard to read at any reasonable zoom level.

**Authors Response:** To make it more clearly, we have updated the Figure 10 with reasonable quality.

**Author's changes in manuscript:** we have enlarged the information in the Figure 10, and the revised Figure 10, in line 398, is shown as follows:

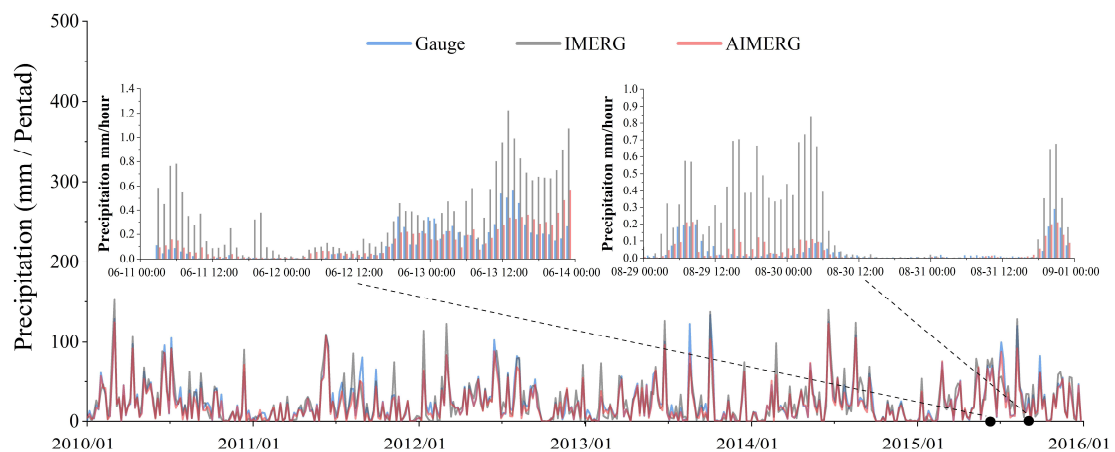


Figure 10. The temporal patterns of mean areal precipitation of IMERG, AIMERG, and the ground observations from the independent hydrological stations, at daily/hourly scale, in Zhejiang province, 2010-2015.

**Point 7:**

**Editor' Comments:** Line 411, Figure 11: No explanation for top three panels (a, b, c).

**Authors Response:** A very good suggestion. To provide more information, we have added a new paragraph, to separately describe the spatial patterns of the ground observations, IMERG, GSMaP, and AIMERG in Figure 11, in lines from 413 to 441.

**Author's changes in manuscript:** To provide more information, we have added a new paragraph, to separately describe the spatial patterns of the ground observations, IMERG, GSMaP, and AIMERG in Figure 11, in lines from 413 to 441. And the content is shown as follows:

In this study, the typhoon, Chan-hom, is selected as an example for assessing the quality of AIMERG and other products, occurred in the typical period 0 a.m., – 11 a.m., July, 11, 2015, in Zhejiang province (Fig. 11 a-d). Generally, the spatial patterns of the IMERG, GSMaP, AIMERG are similar with those of the ground observations, with the increasing volumes of rainfall from southwest to northeast. In terms of the three satellite-based rainfall estimates, IMERG underestimates the rainfall greater than those of GSMaP and AIMERG, in the heavy rainfall events (Fig. 11 b), with largest regions in the southwestern Zhejiang (rainfall < 10 mm/hour). Though GSMaP estimates the rainfall greater than IMERG in both spatial coverages and volumes (Fig. 11 c), the AIMERG provides much more details than GSMaP, especially over the northeastern Zhejiang Province (Fig. 11 c). As pointed out by various studies (e.g., Tang et al., 2020), the satellite-based precipitation products generally overestimate the volumes in small rainfall events, but underestimate the volumes during the heavy rainfall events. From this aspect, AIMERG outperforms the GSMaP as well as the original IMERG, owing to the daily calibrations using the ground observations.

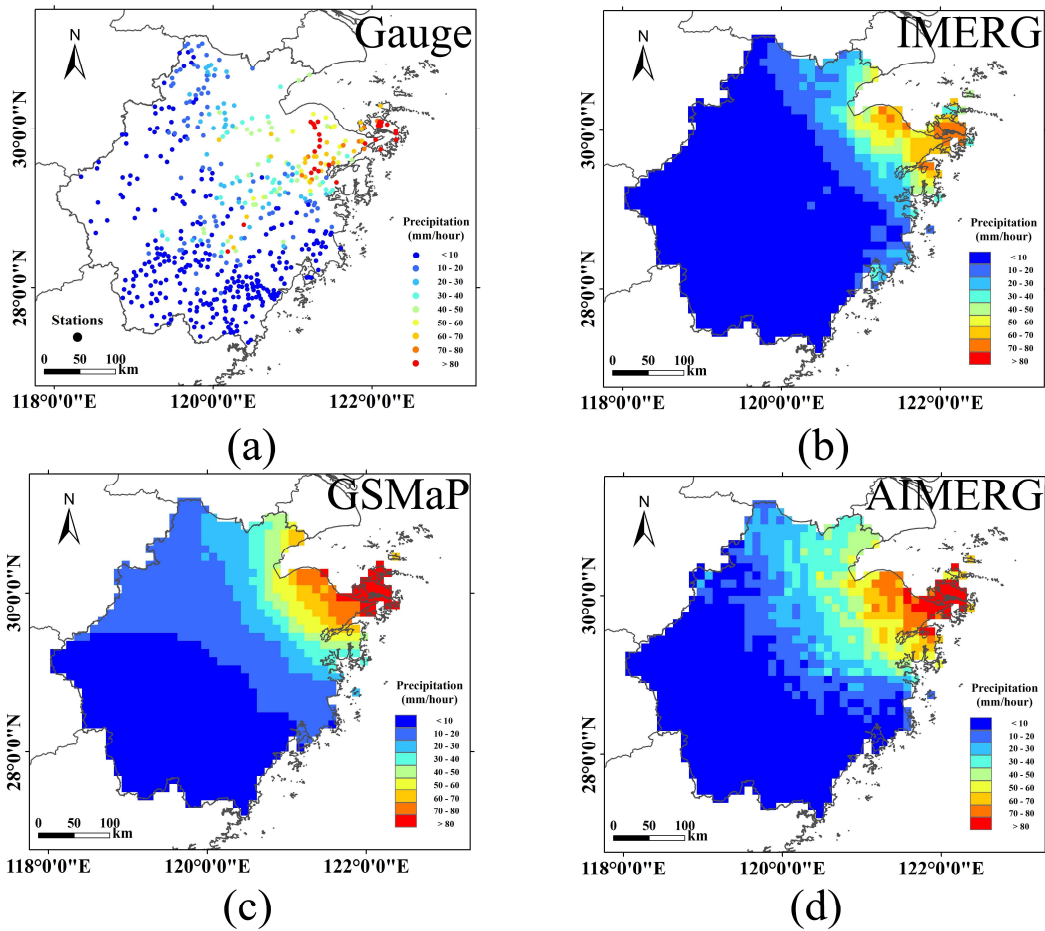


Figure 11. The spatial patterns of precipitation measured by (a) IMERG, (b) GSMaP, and (c) AIMERG, during the typhoon, Chan-hom, occurred in the typical period 0 a.m., – 11 a.m., July, 11, 2015, in Zhejiang Province.

**Point 8:**

**Editor’ Comments:** Line 458, Figure 13: Units for panel c of Figure 13 should be ratio, not mm/month?

**Authors Response:** In Figure 14c, we have replaced the “Precipitation (mm/month)” with “Ratio”.

**Author's changes in manuscript:** In Figure 14c, we have replaced the “Precipitation (mm/month)” with “Ratio”, in line 461.

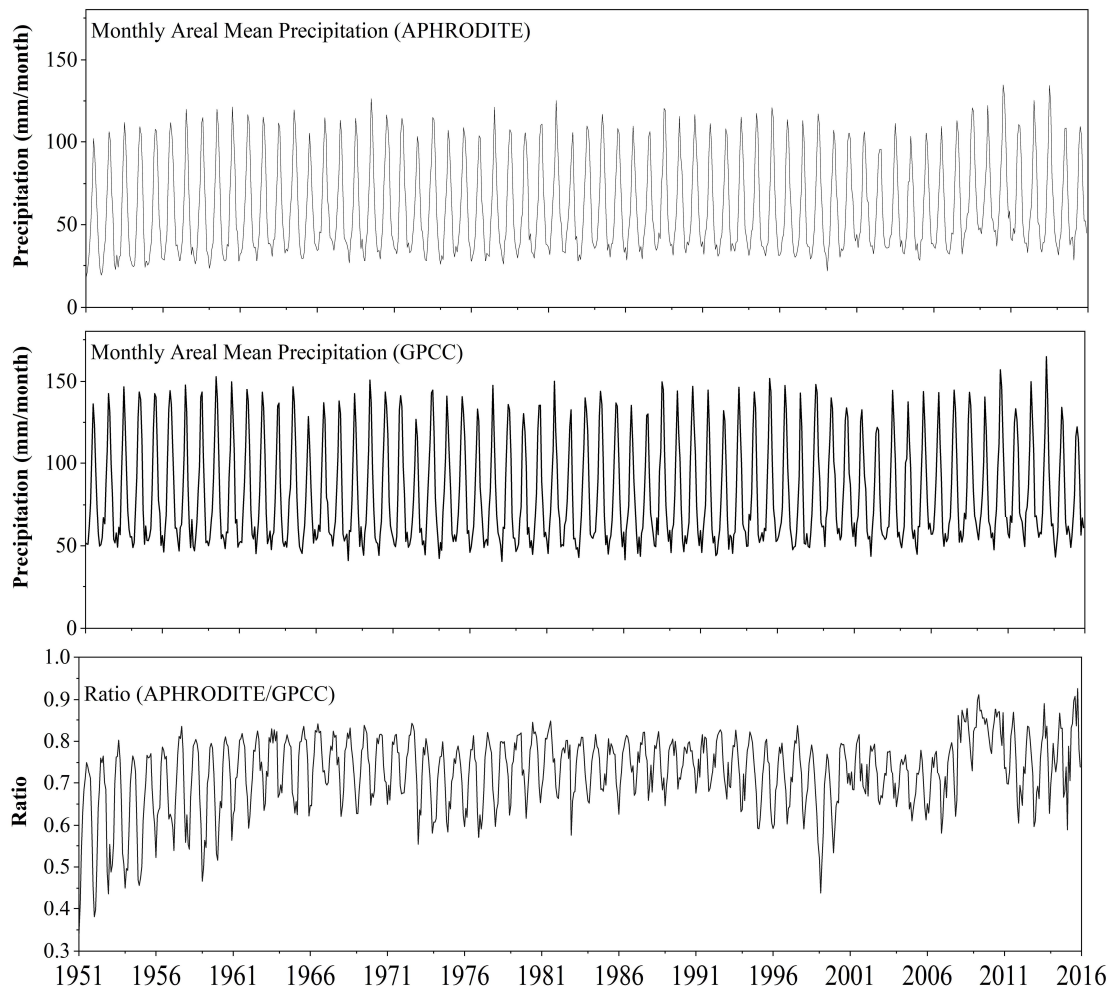


Figure 14. The temporal patterns of monthly areal mean precipitation of (a) APHRODITE and (b) GPCC, and monthly (c) ratio values of corresponding areal mean APHRODITE/GPCC, 1951-2015.

**Point 9:**

**Editor’ Comments:** Line 535, Figure 14: Here a reader needs to go back and forth between Figure 11 and Figure 14 to understand the differences between AIMERG and GSMaP for this particular typhoon. Authors should provide a better, easier comparison?

**Authors Response:** After careful considerations, we have added another subsection in “Result” section, as follows: “4.3. The performances of AIMERG and other products in capturing the heavy rainfall event” in line 401, which considers an easier comparison between AIMERG and GSMaP. And in this new subsection, we have compared the AIMERG with GSMaP, as well as IMERG, in terms spatial patterns (Figure 11) and quantitative volumes (Figure 12), separately.

**Author's changes in manuscript:** After careful considerations, we have provided a new subsection, in lines from 401 to 463, to provide an easier comparison for the readers in comparing the AIMERG

with GSMaP, as well as IMERG. And the newly added content is shown as follows:

#### **4.3. The performances of AIMERG and other products in capturing the heavy rainfall event**

One of the primary aims of the satellite-based precipitation estimates is to provide the high quality rainfall information, accurately capturing both the spatial patterns and volumes of the rainfall, at hourly scale during the heavy rainfall events. Recently, Tang et al (2020) has conducted a comprehensive comparison of GPM IMERG with other nine state-of-the-art high resolution precipitation products, six satellite-based precipitation products (TRMM 3B42, 0.25°/3 hour; CMORPH, 0.25°/3 hour; PERSIANN-CDR, 0.25°/1 day; GSMaP 0.1°/1 hour; CHIRPS, 0.05°/1 day; SM2RAIN, 0.25°/1 day) and three reanalysis datasets (ERA5, ~0.25°/1 hour; ERA-Interim, ~0.75°/3 hour; MERRA2~0.5° × 0.625°/1 hour) from 2000 to 2018, and found that the IMERG product generally outperformed other datasets, except the Global Satellite Mapping of Precipitation (GSMaP), which was adjusted at the daily scale by the gauge analysis (0.5°/daily) from the CPC (Mega et al., 2014). Therefore, we have quantitatively and horizontally compared the AIMERG with GSMaP, as well as the IMERG against ground observations.

In this study, the typhoon, Chan-hom, is selected as an example for assessing the quality of AIMERG and other products, occurred in the typical period 0 a.m., – 11 a.m., July, 11, 2015, in Zhejiang province (Fig. 11 a-d). Generally, the spatial patterns of the IMERG, GSMaP, AIMERG are similar with those of the ground observations, with the increasing volumes of rainfall from southwest to northeast. In terms of the three satellite-based rainfall estimates, IMERG underestimates the rainfall greater than those of GSMaP and AIMERG, in the heavy rainfall events (Fig. 11 b), with largest regions in the southwestern Zhejiang (rainfall < 10 mm/hour). Though GSMaP estimates the rainfall greater than IMERG in both spatial coverages and volumes (Fig. 11 c), the AIMERG provides much more details than GSMaP, especially over the northeastern Zhejiang Province (Fig. 11 c). As pointed out by various studies (Tang et al., 2020), the satellite-based precipitation products generally overestimate the volumes in small rainfall events, but underestimate the volumes during the heavy rainfall events. From this aspect, AIMERG outperforms the GSMaP as well as the original IMERG, owing to the daily calibrations using the ground observations.

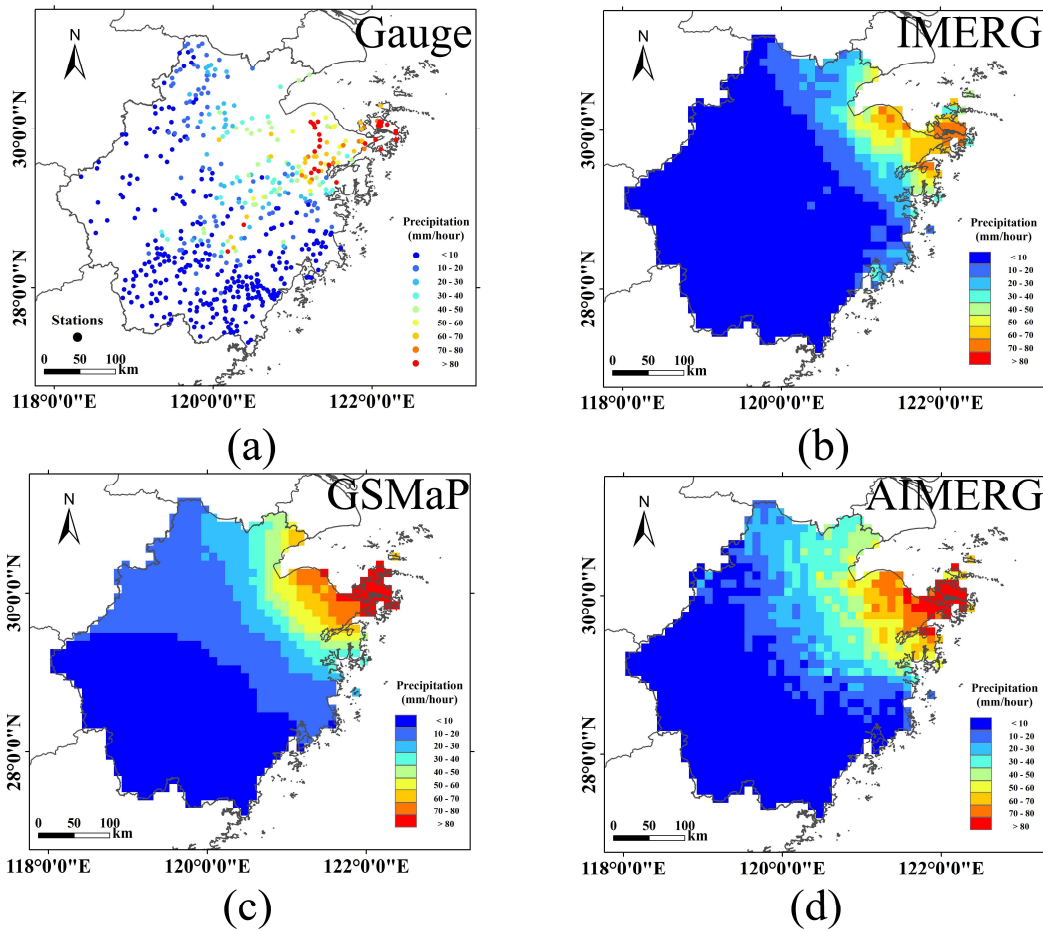


Figure 11. The spatial patterns of precipitation measured by (a) IMERG, (b) GSMaP, and (c) AIMERG, during the typhoon, Chan-hom, occurred in the typical period 0 a.m., – 11 a.m., July, 11, 2015, in Zhejiang Province.

To quantitatively assess the performances of the AIMERG, GSMaP, and IMERG, they are also evaluated against the ground observations, during the typhoon, Chan-hom, occurred in the typical period 0 a.m., – 11 a.m., July, 11, 2015, in Zhejiang province (Fig. 12 a-c). From the statistics, not only the systematic bias of IMERG (around -50%) is significantly improved, with bias of AIMERG around -10%, but also the random errors of IMERG (RMSE ~ 2.7 mm/hour, MAE ~ 1.5 mm/hour) are also reduced, compared with AIMERG (RMSE ~ 2.5 mm/hour, MAE ~ 1.4 mm/hour), which meant the calibrations using APHRODITE on IMERG improved the abilities of original IMERG product to more accurately estimate the quantitative precipitation volumes, especially in heavy rainfall events (Fig. 12 a and c). Meanwhile, AIMERG significantly overwhelms GSMaP in terms of both bias and random errors. For instance, GSMaP underestimates the precipitation (bias ~ -31%) twice as large as AIMERG (bias ~ -15%), and the random errors of GSMaP (MAE ~ 1.97



mm/hour, RMSE ~ 3.26 mm/hour) are also significantly larger than those of AIMERG (MAE ~ 1.44 mm/hour, RMSE ~ 2.50 mm/hour) (Fig. 12 b and c). Compared with the original IMERG, though the random errors of GSMaP are relatively larger, the bias of GSMaP (~ -31%) is significantly smaller than that of the original IMERG (~ -50%), which owes to the calibrations on the GSMaP at the daily scale (Fig. 12 a and b). In future, we also encourage researchers to comprehensively evaluate and compare the AIMERG with other high resolution precipitation products at various spatio-temporal scales.

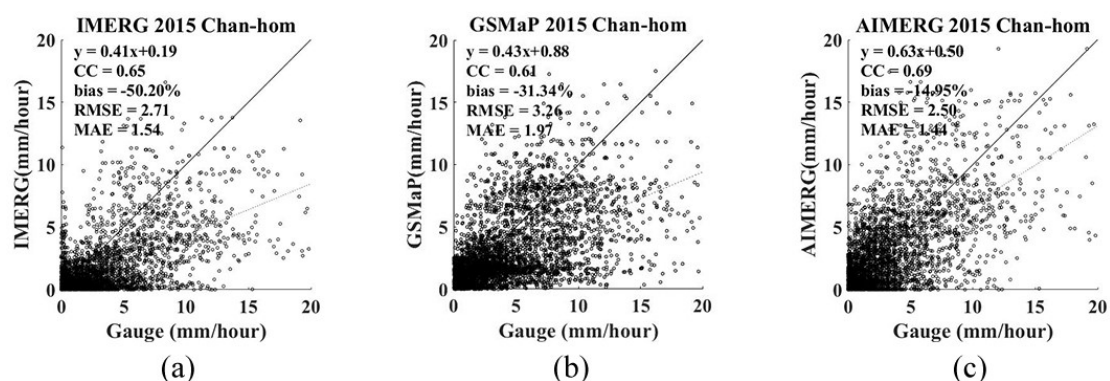


Figure 12. The scatterplots of (a) IMERG, (b) GSMaP, and (c) AIMERG against ground observations during the typhoon, Chan-hom, occurred in the typical period 0 a.m., – 11 a.m., July, 11, 2015, in Zhejiang Province.

**Point 10:**

**Editor’ Comments:** Lines 540 to 542- recommendations for other regions. Readers may agree with this statement but do authors feel confident about availability or quality of high-resolution gauge data for these other regions? For Japan, perhaps yes? Monsoon India, perhaps? Middle East perhaps not? Authors, as regional experts, can provide some guidance here?

**Authors Response:** A very good suggestion, we have provided recommendations for evaluating the AIMERG and other precipitation products for other regions, especially with limited rain gauge networks.

**Author’s changes in manuscript:** we have provided recommendations for evaluating the AIMERG and other precipitation products for other regions, especially with limited rain gauge networks, in lines from 464 to 472. And the content is shown as follows: “The extent of the AIMERG could



cover the Northern Eurasia, Middle East, Monsoon Asia, and Japan. This study mainly evaluated the AIMERG in the China Mainland, which calls for Asia wide evaluations in the future to assess both the algorithm and the corresponding precipitation product. For regions with relative dense rain gauge networks, it is better to quantitatively and horizontally evaluate the AIMERG and other precipitation estimates against ground observations, using statistical evaluations (Lu et al., 201; Xu et al., 2019; Tang et al., 2020), for example, in Japan, and Monsoon India. While for regions with relative sparse rain gauge networks, it is optimal to horizontally compare the performances and abilities of AIMERG with those of other products in precipitation-related application fields, e.g., in hydrological simulations at basin scales (Ma et al., 2018).”

**Point 11:**

**Editor’ Comments:** Page 57, list of acronyms, welcome helpful addition!

**Authors Response:** Thank you very much for your positive comment.

**Point 12:**

**Editor’ Comments:** Difficult, challenging work, requires some final 'smoothing' of language. Overall, a good product for ESSD.

**Authors Response:** Thank you very much for your positive comment. In terms of the remaining **language-based issues**, we will carefully collaborate with Copernicus publishing team during the proof-reading stage, and also would like to consult the **professional English language editing service** (<http://www.sciencemanager.com/>), who has helped us improving several Manuscripts for some other big journals, such as *Remote Sensing of Environment*.

1 **AIMERG: a new Asian precipitation dataset (0.1°/half-hourly, 2000-2015) by calibrating GPM**  
2 **IMERG at daily scale using APHRODITE**

3 Ziqiang Ma<sup>1</sup>, Jintao Xu<sup>2</sup>, Siyu Zhu<sup>1</sup>, Jun Yang<sup>3</sup>, Guoqiang Tang<sup>4,5</sup>, Yuanjian Yang<sup>6</sup>, Zhou Shi<sup>2</sup>, Yang  
4 Hong<sup>1,7</sup>

5 <sup>1</sup>*Institute of Remote Sensing and Geographical Information Systems, School of Earth and Space Sciences, Peking*  
6 *University, Beijing, 100871, China*

7 <sup>2</sup>*Institute of Agricultural Remote Sensing and Information Technology Application, College of Environmental and*  
8 *Resource Sciences, Zhejiang University, Hangzhou, 310058, China*

9 <sup>3</sup>*National Satellite Meteorological Centre, China Meteorological Administration, Beijing, 100081, China*

10 <sup>4</sup>*University of Saskatchewan Coldwater Lab, Canmore, Alberta, Canada, T1W 3G1*

11 <sup>5</sup>*Centre for Hydrology, University of Saskatchewan, Saskatoon, Saskatchewan, Canada, S7N 1K2*

12 <sup>6</sup>*School of Atmospheric Physics, Nanjing University of Information Science and Technology, Nanjing 210044, China*

13 <sup>7</sup>*School of Civil Engineering and Environmental Science, University of Oklahoma, Norman, OK, 73019, United States*

14 Correspondences: Ziqiang Ma ([ziqma@pku.edu.cn](mailto:ziqma@pku.edu.cn)); Prof. Yang Hong ([yanghong@ou.edu](mailto:yanghong@ou.edu))

15

16 **AIMERG: a new Asian precipitation dataset (0.1°/half-hourly, 2000-2015) by calibrating GPM**  
17 **IMERG at daily scale using APHRODITE**

18

19 **Highlights**

20 ● **A new effective daily calibration approach, DSTDCA, for improving GPM IMERG**

21 ● **A new AIMERG precipitation data (0.1°/half-hourly, 2000-2015, Asia) is provided**

22 ● **Bias of AIMERG is significantly improved compared with that of IMERG**

23 ● **APHRODITE is more suitable than GPCC in anchoring IMERG over the Asia**

24

25

26

27

28

29

30

31 **Abstract**

32       Precipitation estimates with fine quality and spatio-temporal resolutions play significant roles in  
33 understanding the global and regional cycles of water, carbon and energy. Satellite-based precipitation  
34 products are capable of detecting spatial patterns and temporal variations of precipitation at fine  
35 resolutions, which is particularly useful over poorly gauged regions. However, satellite-based  
36 precipitation products are the indirect estimates of precipitation, inherently containing regional and  
37 seasonal systematic biases and random errors. In this study, focusing on the potential drawbacks in  
38 generating Integrated Multi-satellitE Retrievals for Global Precipitation Measurement (IMERG) and its  
39 recently updated retrospective IMERG in the Tropical Rainfall Measuring Mission (TRMM) era (finished  
40 in July, 2019), which were only calibrated at monthly scale using ground observations, Global  
41 Precipitation Climatology Centre (GPCC, 1.0°/Monthly), we aim to propose a new calibration algorithm  
42 for IMERG at daily scale, and to provide a new AIMERG precipitation dataset (0.1°/ half-hourly, 2000-  
43 2015, Asia) with better quality, calibrated by Asian Precipitation Highly Resolved Observational Data  
44 Integration (APHRODITE, 0.25°/Daily) at the daily scale for the Asian applications. And the main  
45 conclusions include but not limited to: (1) the proposed daily calibration algorithm (Daily Spatio-  
46 Temporal Disaggregation Calibration Algorithm, DSTDCA) is effective in considering the advantages  
47 from both satellite-based precipitation estimates and the ground observations; (2) AIMERG performs  
48 better than IMERG at different spatio-temporal scales, in terms of both systematic biases and random  
49 errors, over the China Mainland; and (3) APHRODITE demonstrates significant advantages than GPCC

50 in calibrating the IMERG, especially over the mountainous regions with complex terrain, e.g., the Tibetan  
51 Plateau. Additionally, results of this study suggest that it is a promising and applicable daily calibration  
52 algorithm for GPM in generating the future IMERG in either operational scheme or retrospective manner.

53 The AIMERG data record (0.1°/half-hourly, 2000-2015, Asia) is freely available at [http://argi-](http://argi-basic.hihanlin.com:8000/d/d925fecf60/)  
54 [basic.hihanlin.com:8000/d/d925fecf60/](http://argi-basic.hihanlin.com:8000/d/d925fecf60/). Additionally, the AIMERG data is also freely accessible at  
55 <https://doi.org/10.5281/zenodo.3609352> (for the period from 2000 to 2008) (Ma et al., 2020a) and  
56 <http://doi.org/10.5281/zenodo.3609507> (for the period from 2009 to 2015) (Ma et al., 2020b).

57 **Keywords: Precipitation; IMERG; APHRODITE; Calibration; Daily scale; Asia;**

58

## 59 **1. Introduction**

60 Precipitation is among the most essential hydroclimatic factors, and also most difficult to estimate  
61 due to its great small-scale variabilities (Yatagai et al., 2012; Huffman et al., 2019a). High spatio-  
62 temporal resolution precipitation dataset with fine quality is essential for various scientific and  
63 operational applications, including but not limited to driving the hydrological models, and supporting  
64 the predictions of droughts and floods (Beck et al., 2017, 2018). There are mainly two principal  
65 approaches for measuring the global precipitation: ground-based gauge observing, and satellite-based  
66 remote sensing, which resulting in three mainstreams of global precipitation products, namely gauge

67 analysis precipitation data, satellite-based only precipitation estimates, and satellite-gauge combined  
68 precipitation products, based on the consideration that ground-based gauge data are clearly important  
69 for anchoring the satellite estimates (Huffman et al., 2007, 2019a).

70 In recent years, a large number of quasi-global satellite precipitation products with various  
71 temporal and spatial resolutions have been developed and released to the public, such as the PMW-based  
72 CPC Morphing technique (CMORPH) (hereafter, for Acronyms, see the Appendix) (Joyce et al., 2004),  
73 and IR-based PERSIANN (Sorooshian et al., 2000) and PERSIANN-CCS (Hong et al., 2004). As the  
74 milestone in the satellite-based precipitation measurement process, the TRMM and its successor GPM  
75 have developed a flexible framework for generating the most popular precipitation products, TMPA  
76 (1998-present, 0.25°/3 hourly) and IMERG (2014-present, 0.1°/half-hourly), as well as the retrospective  
77 IMERG (2000-present, 0.1°/half-hourly) from GPM era to TRMM era, which aim~~sed~~ at intercalibrating,  
78 merging, and interpolating all MW estimates of the GPM constellation, IR estimates, and gauge  
79 observations (Huffman et al., 2019b). The “Final run” version of IMERG (hereafter refer to IMERG),  
80 incorporating the monthly gauge analysis, provides the state-of-the-art precipitation estimate with finest  
81 spatio-temporal resolutions so far, while it still contains large uncertainties, e.g., greatly overestimating  
82 the precipitation, at daily and hourly scales from regions to regions, especially over the mountainous  
83 areas, such as the Tibetan Plateau, China (Tang et al., 2016; Lu et al., 2019; Xu et al., 2019), which is  
84 greatly potentially resulted by the calibration procedures in the process of generating the IMERG.  
85 Currently, the IMERG product (following the gauge correction method of TMPA approach) (Huffman

86 et al., 2007) has been produced by anchoring the multi-satellite-only precipitation estimates using the  
87 monthly analysis Satellite-Gauge product (1.0°/monthly, 1979 to the present, delayed by about 3 months)  
88 from the GPCC (Adler et al., 2003, 2018), therefore, the IMERG performed better at monthly and annual  
89 scales than those at finer temporal scales (e.g., daily, hourly).

90 Satellite-based precipitation products have significant advantages in detecting the variations of  
91 precipitation at fine spatio-temporal resolutions, especially over the poorly gauged regions. However, as  
92 the indirect estimates of precipitation, satellite-based precipitation products are inherently containing  
93 regional, seasonal, and diurnal systematic biases and random errors (Ebert et al., 2007), which could be  
94 effectively alleviated by anchoring the satellite-only precipitation products using gauge-based  
95 observations (Huffman et al., 2007). Therefore, great efforts have been taken on exploring the calibrations  
96 on the satellite-only precipitation estimates using gauge analysis. Historically, GPCP has provided the  
97 lion's share of the early efforts in the process of developing calibration algorithms for the satellite-only  
98 precipitation estimates in generating SG products (2.5°/monthly). For instance, to correct the bias of the  
99 multi-satellite only estimates (mainly based on PMW and IR data) on a regional scale, the multi-satellite  
100 estimate was firstly multiplied by the ratio of the large-scale (with moving window size  $5 \times 5$ ) average  
101 gauge analysis to the large-scale average of the multi-satellite estimate, and then the SG estimate was  
102 finally derived by combining the gauge-adjusted multi-satellite estimate and the gauge analysis with  
103 inverse-error-variance weighting (Huffman et al., 1997; Adler et 2003; Adler 2018). Recently, a two-step  
104 strategy was proposed to remove the bias inherent in the multi-satellite only precipitation estimates using

105 PDF matching method and to combine the bias-corrected estimates with the gauge analyses using OI  
106 algorithm (Xie and Xiong, 2011; Shen et al., 2014). And a similar improved PDF algorithm was applied  
107 to generate the GSMaP data, which was adjusted at the daily scale by the gauge analysis (0.5°/daily) from  
108 the CPC (Mega et al., 2014). While GPM IMERG adjusted the multi-satellite precipitation estimates  
109 (0.1°/half hourly) at the monthly scale using the ratios between the original monthly multi-satellite-only  
110 and the monthly satellite-gauge data, in combination with the original monthly multi-satellite-only and  
111 GPCC (1.0°), in the month (Huffman et al., 2019a). There is still much room for exploring the improved  
112 algorithms for calibrating the multi-satellite-only precipitation estimates at finer spatiotemporal scales, e.  
113 g, 0.25°/daily, which is also one of the next vital focuses by the GPM (Huffman et al., 2019a).

114 As for anchoring the satellite precipitation estimates, the quality and spatio-temporal resolutions of  
115 the gauge analysis precipitation data are the key factors. Though the GPCC has developed a series of  
116 gauge-based precipitation analysis datasets with the quality and spatio-temporal resolutions continually  
117 improved, accurate estimations of precipitation over the land are still greatly difficult with limited  
118 networks of rain gauges. In Asia, great efforts also have been mainly paid on generating gauge-analysis  
119 precipitation products at the monthly scale (Chen et al., 2002; Mitchell and Jones 2005; Matsuura and  
120 Willmott 2009; Schneider et al. 2008), and limited explorations at the daily scale, e.g., Rajeevan and  
121 Bhate (2009) explored daily grid precipitation data over India with data from more than 2,500 rain  
122 gauges. Meanwhile, significant differences among those products ~~had~~have been reported by Yatagai et  
123 al (2005, 2012). To more accurately monitor and predict the Asian hydro-meteorological environment,



124 the APHRODITE project (starting in 2006) aimed at developing the state-of-the-art gridded precipitation  
125 datasets at the resolutions of 0.25°/daily covering the entire Asia based on the largest numbers of ground  
126 observations from multi-sources. Since the release of APHRODITE products (1951-2015, 0.25°/daily,  
127 Last update October 5, 2018), APHRODITE daily grid precipitation data sets have been widely used,  
128 and it distinguished from other gauge analysis data by considering the different interpolation schemes  
129 and climatology characteristics, especially over the mountainous regions with complex terrain, e.g., the  
130 Tibetan Plateau (Yatagai et al., 2012).

131 The aim of this study is to explore the calibration approach at daily scale on the retrospective  
132 IMERG data using APHRODITE product, in both TRMM and GPM eras, from 2000 to 2015.  
133 ~~Therefore~~Meanwhile, a new calibration approach, Daily Spatio-Temporal Disaggregation Calibration  
134 Algorithm (DSTDCA), is proposed and suggested for the GPM in their future algorithms; ~~and~~  
135 meanwhile, a new AIMERG precipitation dataset (0.1°/ half-hourly, 2000-2015, Asia) (Ma et al., 2020a,  
136 b) with better quality is to be provided publicly for the Asian applications.

## 137 2. Data

### 138 2.1 IMERG

139 To generate the IMERG product, IMERG ~~focused~~focuses on intercalibrating, merging, and  
140 interpolating “all” satellite MW-based precipitation estimates, together with MW-calibrated IR-based  
141 precipitation estimates, precipitation gauge analyses, and potentially other precipitation estimators at

142 fine spatio-temporal scales for the both TRMM and GPM eras over the entire globe. Currently, IMERG  
143 is at its Version 06 stage  
144 ([https://pmm.nasa.gov/sites/default/files/document\\_files/IMERG\\_ATBD\\_V06.pdf](https://pmm.nasa.gov/sites/default/files/document_files/IMERG_ATBD_V06.pdf)), based on which  
145 IMERG has been retrospect to the TRMM era at the end of September, 2019, and IMERG is now  
146 available back to June 2000 (~~half-hourly~~0.1°/0.1°~~half-hourly~~) ([https://pmm.nasa.gov/data-](https://pmm.nasa.gov/data-access/downloads/gpm)  
147 [access/downloads/gpm](https://pmm.nasa.gov/data-access/downloads/gpm)). The “Final run” of IMERG combines the GPCP Monitoring product, the V8  
148 Full Data Analysis for the majority of the time (currently 1998-2016), and the V6 Monitoring Product  
149 from 2017 to the then-present. The Monitoring Product is posted about two months after the month of  
150 observations from ~7,000-8,000 stations world-wide, which is relative sparse, especially over the Asia  
151 (Schneider et al. 2014, 2018).

## 152 2.2 APHRODITE

153 Since the release of the APHRODITE product (0.25°/Daily, 1951-2007), it has been widely used as  
154 one of state-of-the-art daily grid precipitation datasets over the Asia, for hydro-climatological related  
155 studies (Yatagai et al., 2012; Menegoz et al., 2013; Sunilkumar et al., 2019). APHRODITE has been  
156 demonstrated to replicate ‘ground truth’ observations very well (Duncan and Bigg, 2012) and represents  
157 the optimal dataset for analyzing historical precipitation variability and change. Recently, the  
158 APHRODITE data has been updated from the former period 1951-2007 to a longer period 1951-2015, in  
159 September, 2018, with continuous efforts of quality control (QC) flagging some data (Hamada et al.,

160 2011). The APHRODITE data could be available through the website (<http://aphrodite.st.hirosaki->  
161 [u.ac.jp/download/](http://aphrodite.st.hirosaki-u.ac.jp/download/)).

## 162 **2.3 CMPA**

163 The China Merged Precipitation Analysis (CMPA, 0.1°/hourly, 2008-2015) ~~were~~ has been generated  
164 by using hourly rain gauge data at more than 30, 000 automatic weather stations in China, with the  
165 combination of the CMORPH precipitation product, and provided by the Chinese Meteorological  
166 Administration (<http://data.cma.cn>) (Shen et al., 2014). The OI method was adopted to estimate the areal  
167 precipitation distribution based on the gauge observations (Yong et al., 2010), but relative large  
168 uncertainty still exists in the interpolated precipitation field particularly over West-western China with  
169 relatively sparse gauge networks. For grid boxes with gauges, the observed precipitation values are  
170 exactly the gauge observations or the averaged observations when more than one gauge locates in a grid.

## 171 **2.4 Point-based rain gauge data from meteorological stations**

172 The hourly rain gauge datasets from 57, 835 national ground stations used in this study, in 2015,  
173 were collected from the National Meteorological Information Center of CMA (<http://data.cma.cn>). All  
174 the gauge data have undergone strict quality control in three levels, which includes (1) the extreme values'  
175 check, (2) internal consistency check, and (3) spatial consistency check (Shen et al., 2010). Most gauges  
176 are located over the eastern and southern parts of the Mainland China, and relatively sparse gauge  
177 networks are located across the northern and western parts, especially over the Tibetan Plateau. The

178 limited number of gauges could be a source of error in evaluation of satellite precipitation products in  
179 such areas (Shen et al., 2014).

## 180 **2.5 Point-based rain gauge data from hydrological stations**

181 The hourly ground precipitation observations from around 500 hydrological stations (the number of  
182 station varied from year to year) used in this study were collected from Hydrology Bureau of Zhejiang  
183 Province, southeastern China (<http://data.cma.cn/>). The quality control follows two steps: (1) the datasets  
184 are filtered by threshold value after being collected from rain gauges; (2) the outliers are identified through  
185 manual processing. With careful data quality control, the rain gauge datasets have satisfying performances  
186 on the accuracy and validity.

187 There are five datasets used in this study (refer to Table 1 for a summary of the datasets).- IMERG  
188 and APHRODITE ~~were~~have been used for generating the AIMERG data, and the others have been~~were~~  
189 used for evaluating and comparing the IMERG and AIMERG at different scales.

190

191 **Table 1.** List of satellite-based, gauge-based, and satellite-gauge combination precipitation products used  
 192 in this study.

Short name	Full name	Spatial and temporal sampling	Time period	References
IMERG	Integrated Multi-satellitE Retrievals for Global Precipitation Measurement	0.1°/half-hourly	2000- <del>present</del> 2015	Huffman et al. (2019b) <a href="https://pmm.nasa.gov/data-access/downloads/gpm">https://pmm.nasa.gov/data- access/downloads/gpm</a> (last access: 17 January 2020)
	Asian Precipitation Highly Resolved Observational Data			
APHRODITE	Integration Towards Evaluation of Water Resources	0.25°/daily	1951-2015	Yatagai et al. (2012) <a href="http://aphrodite.st.hirosaki-u.ac.jp/download/">http://aphrodite.st.hirosaki- u.ac.jp/download/</a> (last access: 17 January 2020)
CMPA	China Merged Precipitation Analysis	0.1°/hourly	2008- <del>present</del> 2015	Shen et al. (2014) <a href="http://data.cma.cn">http://data.cma.cn</a> (last access: 17 January 2020)
	Point-based rain gauge data <a href="#">from meteorological stations</a>			hourly
	<a href="#">Point-based rain gauge data from hydrological stations</a>	hourly	<del>2010-</del> 2015	<a href="#">Shen et al. (2010)</a> <a href="http://data.cma.cn">http://data.cma.cn</a> (last access: 17 January 2020)

193

194 **3. Methodology**

### 3.1 Calibration Procedure of the Daily Spatio-Temporal Disaggregation Calibration

#### Algorithm, DSTDCA

According to previous evaluations on IMERG (Lu et al., 2019; Xu et al., 2019), there are at least two characteristics resulting its significant overestimations: (1) the amplitude of hourly or half-hourly estimated rainfall rates are significantly amplified by IMERG compared with ground observations, which might be caused by the benchmark of GPCC and GPCP SG data for calibrations, and (2) the IMERG algorithm is generally over detecting precipitation events, resulting a large fraction of false alarm but unreal precipitation events. Therefore, this study selects the APHRODITE data as the benchmark for calibrating IMERG at daily scale, based on the proposed approach, DSTDCA, and the main steps of the DSTDCA are shown as follows:

(1) IMERG data ( $0.1^\circ$ /half-hourly) are accumulated to IMERG data at the daily scale ( $0.1^\circ$ ), which are used to generate the spatial disaggregation weights. As the spatial resolution of APHRODITE data is  $0.25^\circ$ , the moving window size of 3 by 3 is selected, and the daily spatial disaggregation weights ( $0.1^\circ$ ) based on IMERG is obtained by calculating the ratios between the daily rainfall accumulations at the central grid and the average daily rainfall accumulations in the corresponding  $3 \times 3$  window. The daily spatial disaggregation weights consider the relative spatial patterns of the precipitation captured by the IMERG;

212 (2) Based on the daily precipitation accumulations of IMERG, the half-hourly temporal  
213 disaggregation weights ( $0.1^\circ$ ) are derived by calculating the ratios between the each half-hourly  
214 precipitation estimates and the corresponding daily precipitation estimates. If the daily accumulation  
215 estimate is equal to zero, then each half-hourly temporal disaggregation weight is set as zero;

216 (3) As there is a small fraction of grids in APHRODITE with no data at daily scale, the no data grids  
217 in APHRODITE data are firstly filled with the data according to its nearest neighbor with effective value;

218 (4) Spatial calibrations: the daily calibrated IMERG using APHRODITE data are obtained by  
219 multiplying the spatial disaggregation weights based on IMERG ( $0.1^\circ/\text{daily}$ ) from step (1) by daily  
220 APHRODITE data ( $0.25^\circ/\text{daily}$ ) from step (3). In this step, to match the IMERG ( $0.1^\circ$ ) and APHRODITE  
221 ( $0.25^\circ$ ), the numbers and weights of the APHRODITE grids corresponding to each IMERG pixel are  
222 determined, according to the relative spatial locations and coverage relationships between the each pixel  
223 of IMERG ( $0.1^\circ$ ) and the corresponding pixels of APHRODITE ( $0.25^\circ$ );

224 (5) Temporal calibrations: the half-hourly calibrated IMERG are obtained by multiplying the half-  
225 hourly temporal disaggregation weights ( $0.1^\circ/\text{half-hourly}$ ) from step (2) by the daily calibrated IMERG  
226 from step (4);

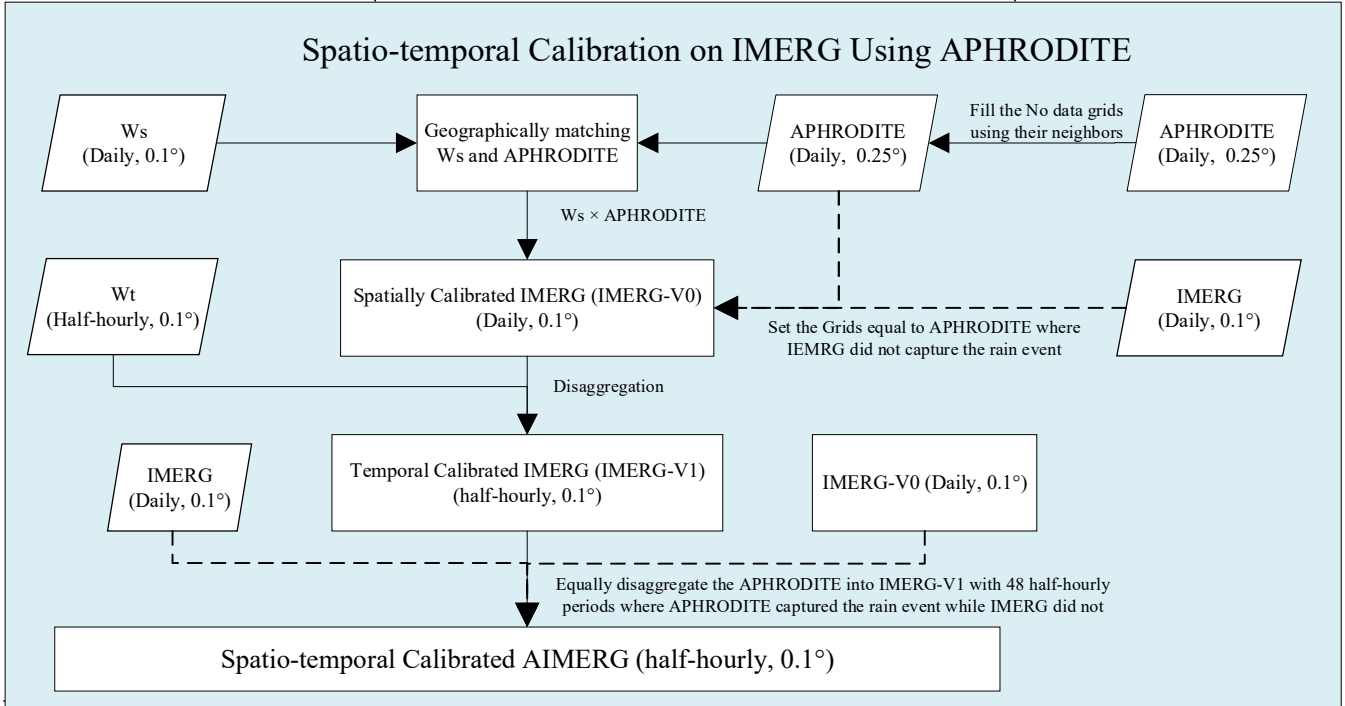
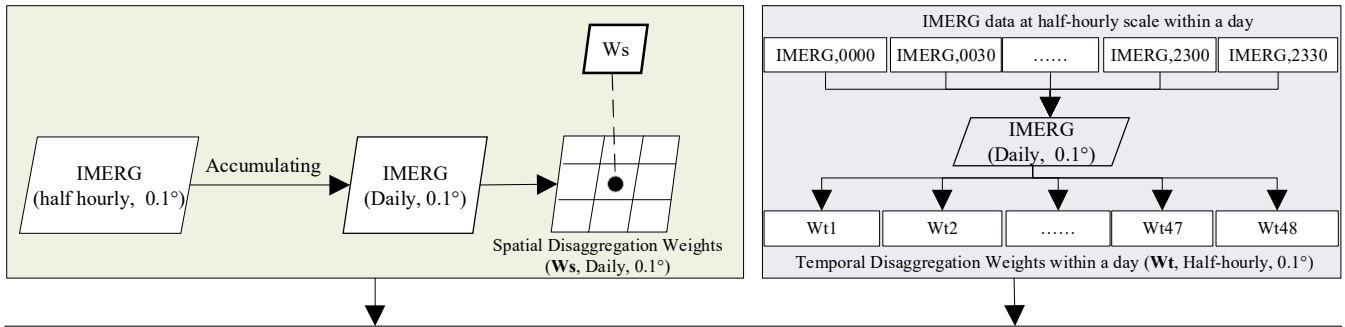
227 (6) By considering the situations that APHRODITE data captured the precipitation while the IMERG  
228 did not, the half-hourly calibrated IMERG is further processed by equally disaggregating the value from

229 the daily APHRODITE data at the corresponding grid into 48 half-hourly periods, which are regarded as  
230 the half-hourly calibrated IMERG values in the corresponding day;

231 (7) By considering the situations that IMERG data captured the precipitation while the APHRODITE  
232 did not, the 48 half-hourly calibrated IMERG values in corresponding days and locations are all set as  
233 zero values, to meet the ground truth observations. And this consideration has been already conducted in  
234 the fourth-step (4);

235 After all the above-mentioned procedures, the final calibrated AIMERG (0.1° half-hourly) data are  
236 obtained by considering both the total precipitation controls and the effective precipitation events  
237 measured by the “ground truth” observations by APHRODITE data over the Asia. And the flowchart of  
238 the Daily Spatio-Temporal Disaggregation Calibration Algorithm, DSTDCA, could be clearly seen in  
239 Figure 1.





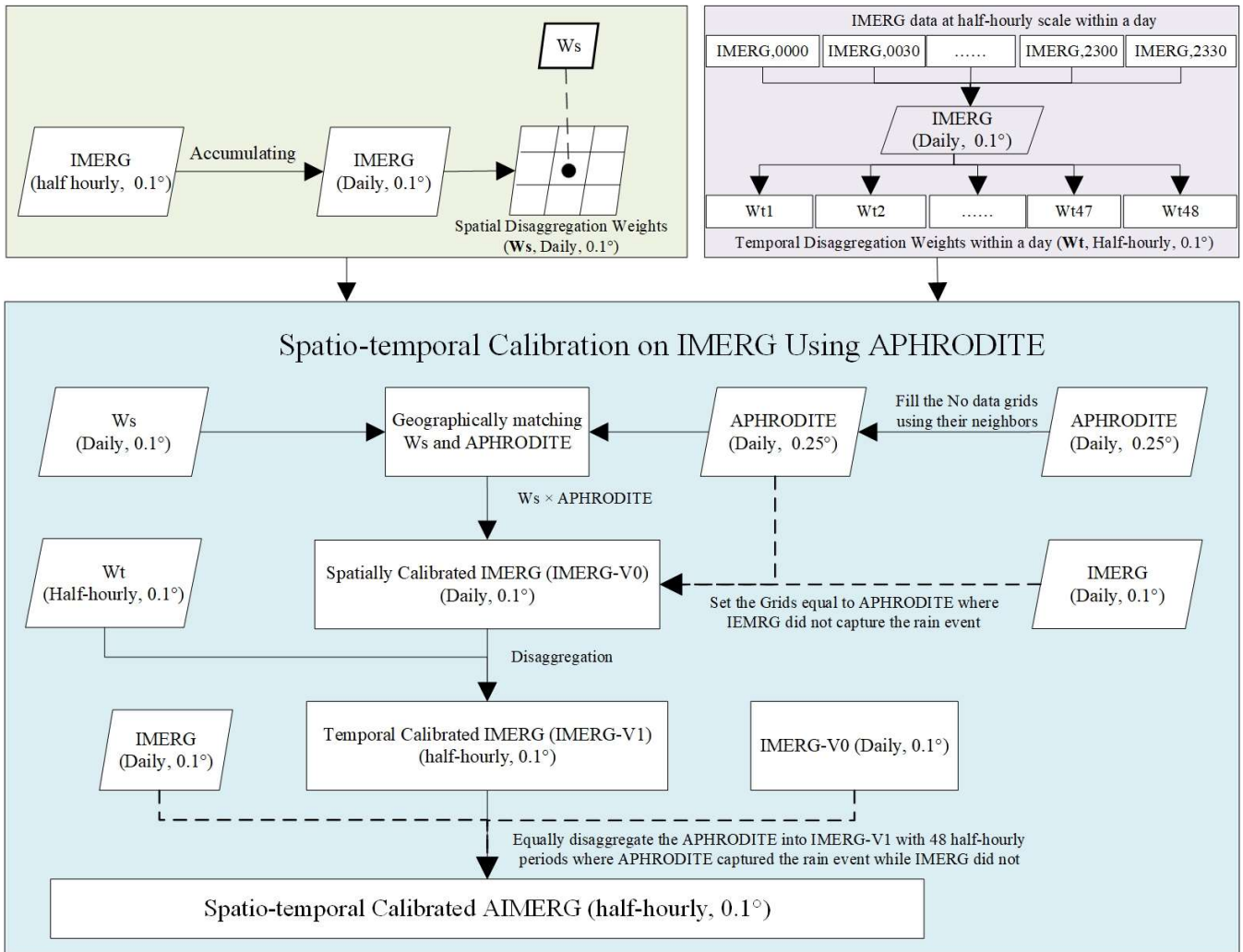


Figure 1. The flowchart of the Daily Spatio-Temporal Disaggregation Calibration Algorithm, DSTDCA, to generate the AIMERG dataset over the Asia, 2000-2015

### 3.2 Evaluation Metrics

246 To evaluate the IMERG and its calibrations comprehensively, seven metrics (CC, MAE, BIAS,  
 247 RMSE, POD, FAR, CSI) were selected [in this study](#) (Tang et al., 2016). Generally, CC is used to describe  
 248 the agreements between satellite estimates and gauge observations; MAE, RMSE, and BIAS are used to  
 249 indicate the error and bias of satellite estimates compared with gauge observations; and the POD, FAR,  
 250 and CSI are used to demonstrate the capabilities to correctly capture the precipitation events of satellite  
 251 precipitation estimates against the ground observations. The detailed information of these evaluation  
 252 metrics are listed in Table 2.

253 **Table 2** Formulas and perfect values of the evaluation metrics used in this study<sup>a</sup>.

Statistic metrics	Equation	Perfect value	Value ranges
Correlation Coefficient (CC)	$CC = \frac{\frac{1}{N} \sum_{n=1}^N (S_n - \bar{s})(G_n - \bar{G})}{\sigma_S \sigma_G}$	1	[-1, 1]
Mean <u>Absolute</u> Error (MAE)	$MAE = \frac{1}{N} \sum_{n=1}^N ( S_n - G_n )$	0	( <del>-∞</del> 0, +∞∞)
Relative Bias (BIAS)	$BIAS = \frac{\sum_{n=1}^N (S_n - G_n)}{\sum_{i=1}^n G_n} \times 100\%$	0	(-∞, +∞)
Root Mean Square Error (RMSE)	$RMSE = \sqrt{\frac{1}{N} \sum_{n=1}^N (S_n - G_n)^2}$	0	[0, +∞)
Probability of Detection (POD)	$POD = \frac{n_{11}}{n_{11} + n_{01}}$	1	[0, 1]
False Alarm Ratio (FAR)	$FAR = \frac{n_{10}}{n_{11} + n_{10}}$	0	[0, 1]
Critical Success Index (CSI)	$CSI = \frac{n_{11}}{n_{11} + n_{10} + n_{01}}$	1	[0, 1]

254 <sup>a</sup>Notation: n is the sample numbers; S<sub>n</sub> is satellite precipitation estimate; G<sub>n</sub> is gauge-based precipitation; σ<sub>G</sub> is the standard deviations of  
 255 gauge-based precipitation; σ<sub>S</sub> is the standard deviations of satellite-based precipitation estimate. n<sub>11</sub> is the precipitation event detected by  
 256 both gauge and satellite simultaneously; n<sub>10</sub> is the precipitation event detected by the satellite but not detected by the gauge; n<sub>01</sub> is contrary  
 257 to n<sub>10</sub>; n<sub>00</sub> is the precipitation events detected neither by the gauge nor the satellite.

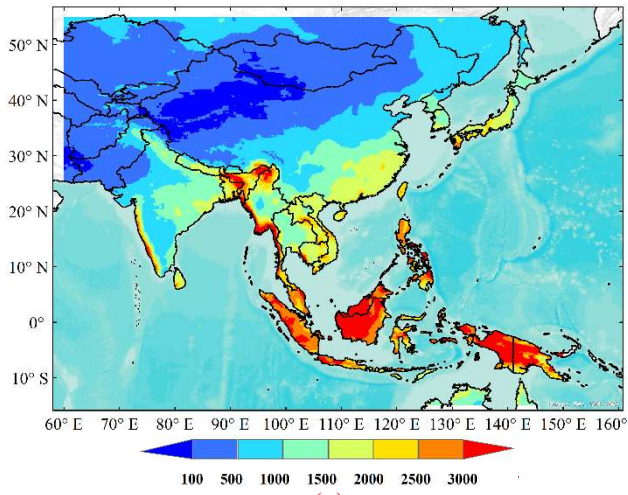
258

## 259 4. Results

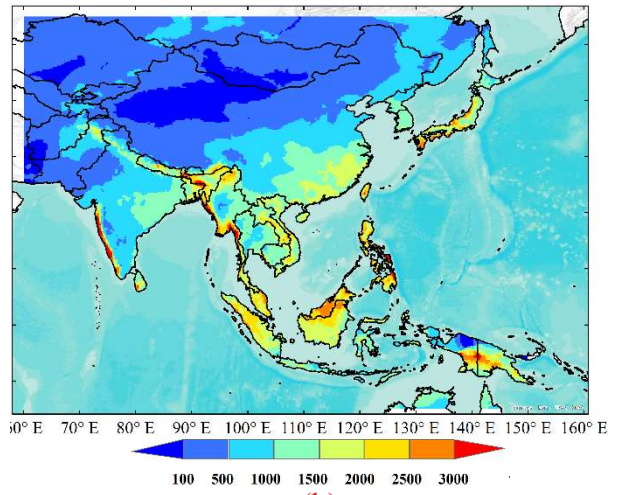
### 260 4.1 AIMERG Product

261 Generally, both IMERG and APHRODITE share similar spatial patterns with precipitation volumes  
262 decreasing from southeast to northwest in Asia, while compared with APHRODITE data (Fig. 2b),  
263 IMERG greatly overestimates the precipitation over Arunachal Pradesh, coastal Indochina and Western  
264 Ghats, and the Indonesia (Fig. 2a). Corrected by APHRODITE, the spatial patterns and volumes of  
265 AIMERG are much more similar to those of APHRODITE, especially along the Himalayas, coastal  
266 Indochina and Western Ghats, and the Indonesia (Fig. 2c). Compared with APHRODITE, AIMERG  
267 seems floating up and down in terms of the volumes, for instance, AIMERG is larger and smaller than  
268 APHRODITE in eastern Indonesia and northeastern Asia, respectively. —Though AIMERG is smaller  
269 than IMERG over most regions, there are still some areas where the volumes of AIMERG are larger than  
270 those of IMERG, e.g., in western Tibetan Plateau, ~~Middle East, and along the western coast of India~~ (Fig.  
271 2d).

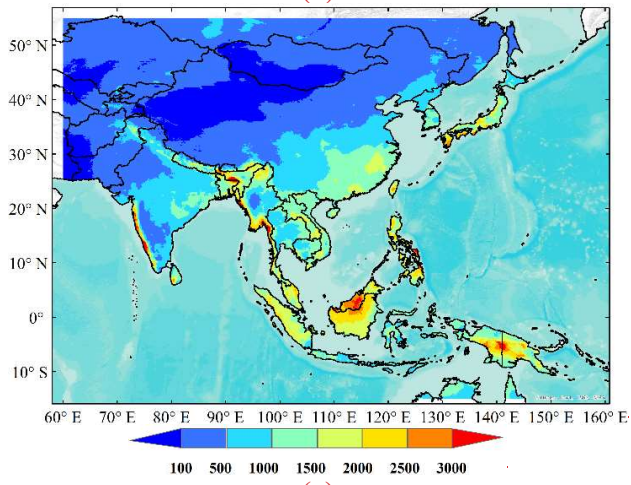
272



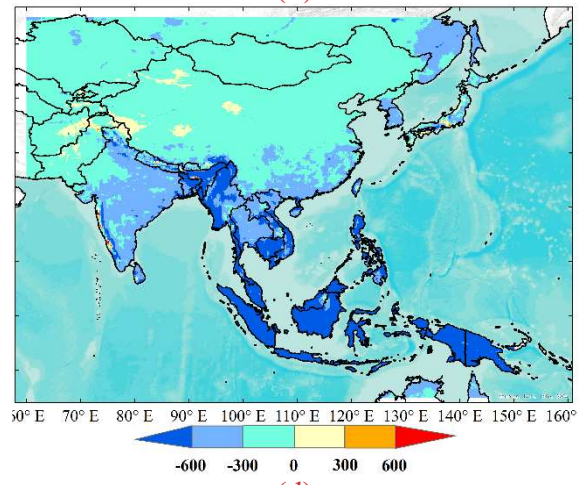
(a)



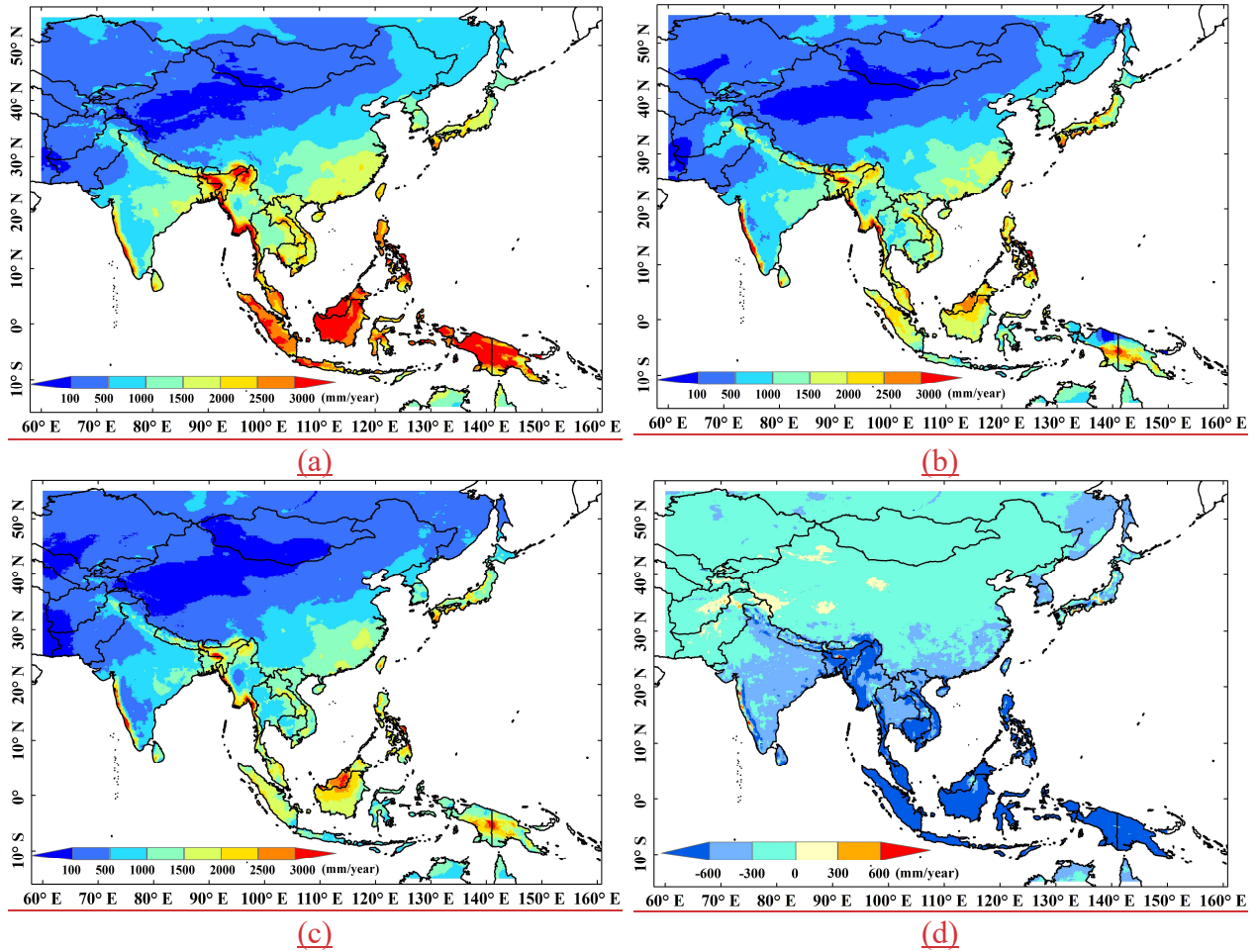
(b)



(c)



(d)

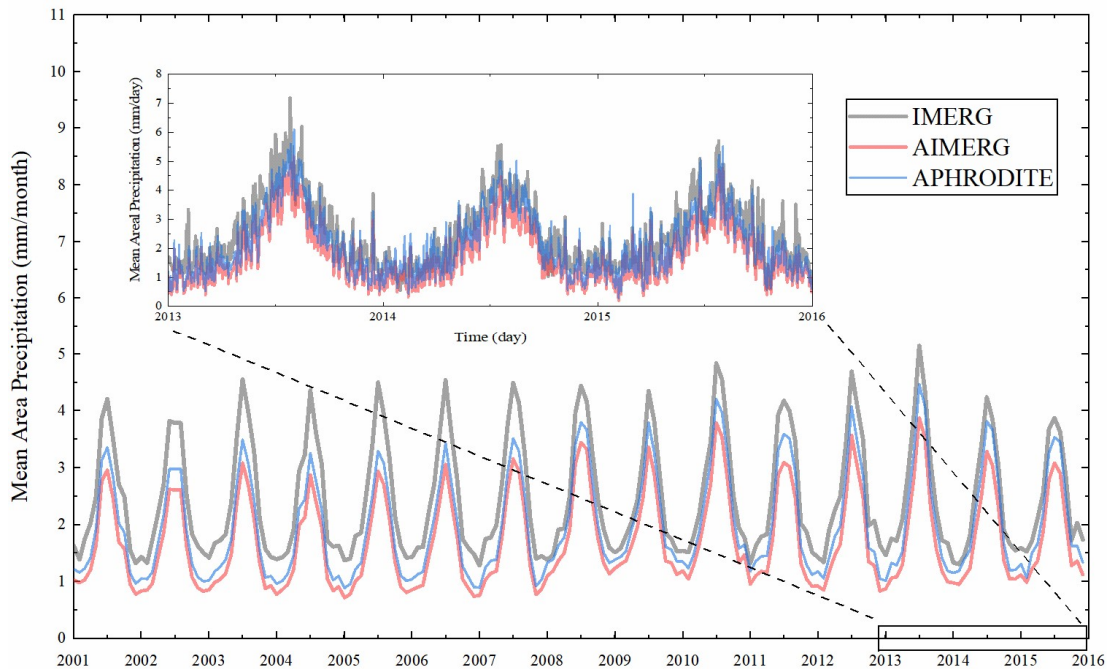


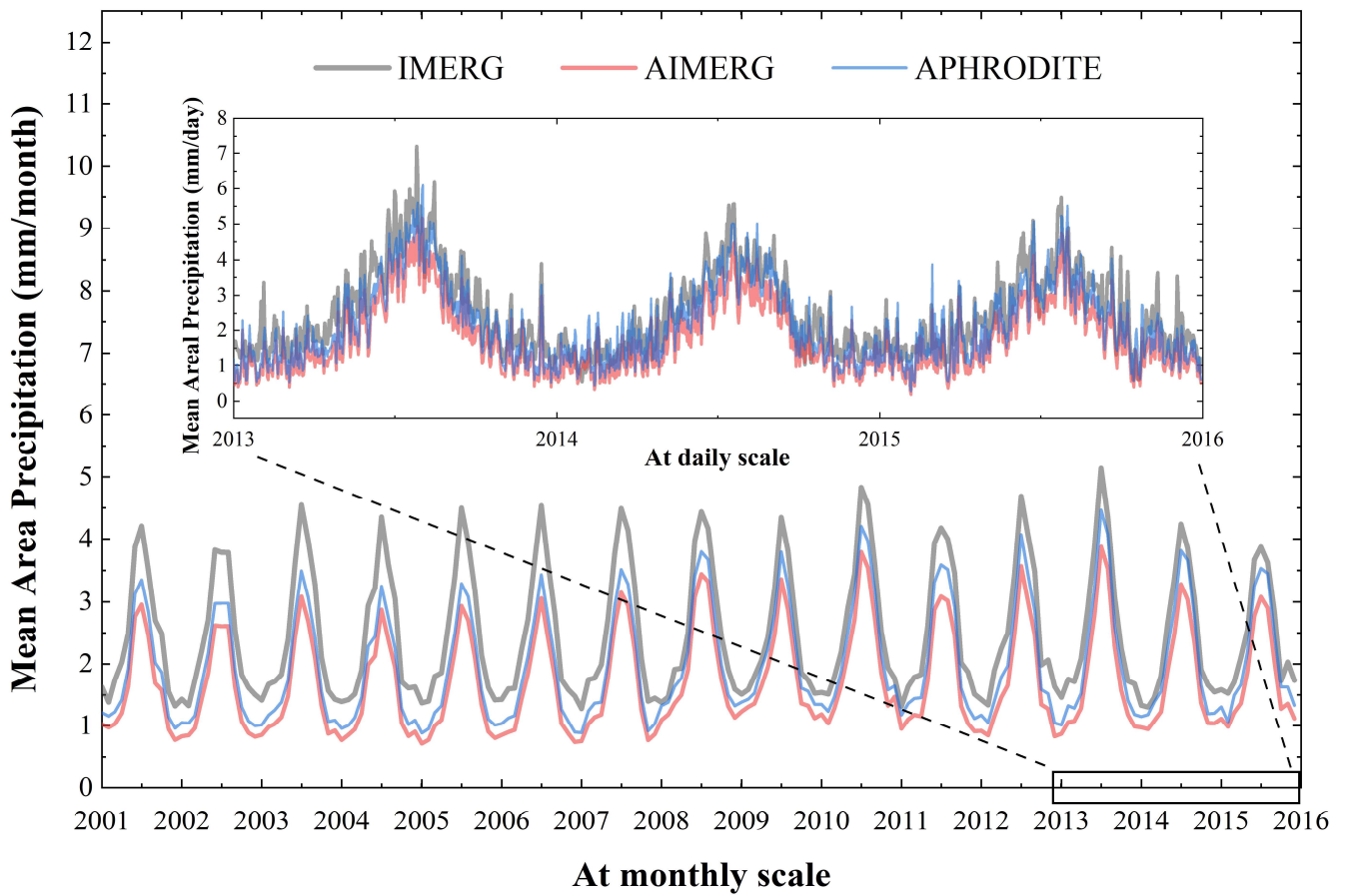
273 Figure 2. Spatial patterns of Asian mean annual gridded precipitation products of (a) IMERG, 0.1°, (b)  
 274 APHRODITE, 0.25°, and (c) AIMERG, 0.1°, and (d) AIMERG-IMERG, 0.1°, respectively, during the  
 275 period of 2001-2015. ~~The background map used in this study was provided by Esri, USGS and NOAA~~  
 276 ~~([http://goto.arcgisonline.com/maps/World\\_Terrain\\_Base](http://goto.arcgisonline.com/maps/World_Terrain_Base), last access: 17 January 2020).~~

277



278 The temporal patterns of the mean areal precipitation over the Monsoon Asia of the three products  
279 demonstrate that the systematic bias of IMERG is significantly reduced in both dry and wet seasons,  
280 shown in Fig. 3. IMERG is around 1.5 times larger than APHRODITE at monthly scale. Though much  
281 more close to the APHRODITE, AIMERG is still a little smaller than the APHRODITE, which means  
282 the calibration algorithm proposed by this study tends to underestimate the precipitation compared with  
283 calibration benchmark, APHRODITE. At daily scale, IMERG is generally larger than APHRODITE,  
284 while at some special days, APHRODITE is larger than IMERG, which might result the AIMERG may  
285 be also larger than IMERG.





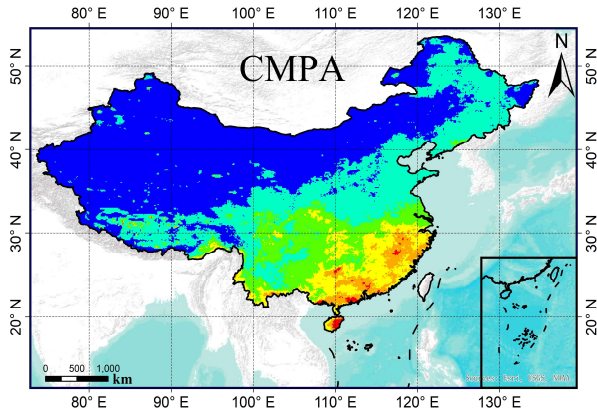
286 Figure 3. The temporal variations of mean Asian gridded precipitation products of IMERG, APHRODITE,  
 287 and AIMERG, respectively, during the period of 2001-2015.

288 **4.2 Assessments on IMERG and AIMERG at national and regional scales**

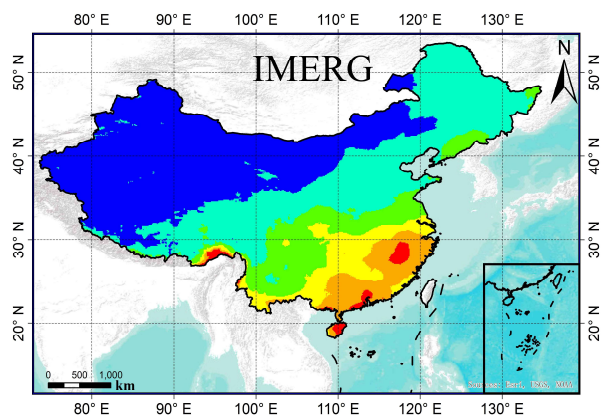
289 The spatial patterns of CMPA demonstrate much more similar to those of AIMERG, especially in  
 290 the southeastern China where dense rain gauges are located, while both CMPA and IMERG overestimate  
 291 the precipitation along the Himalayas where the meteorological gauges are sparse and mainly the satellite-



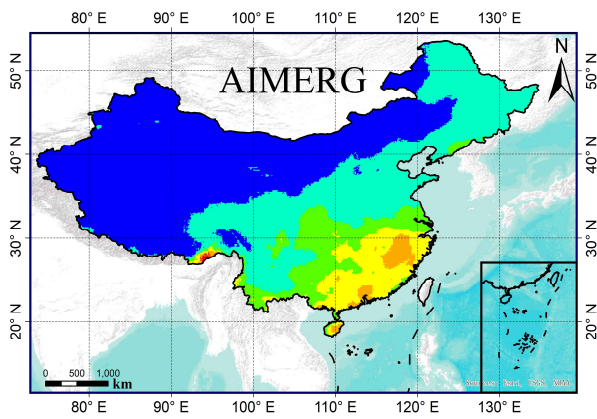
292 based observations are applied (Fig. 4). Obviously, the IMERG significantly overestimates the  
293 precipitation in the southeast coast of China, where typhoons always visit (Fig. 4 b). For deciding the  
294 sub-regions (Fig. 4 d), we have mainly considered three aspects: the representative climatic zones in  
295 China, the local distributions of the gauge stations, and the complexity of the topography. For instances,  
296 Sub-Region 1 represents the high latitude plain in the most north-eastern region of China under a cold  
297 climate (left top: 115.0° E, 54.0°N; right bottom: 135.0° E, 47.0°N); Sub-Region 2 represents the south-  
298 eastern coastal area of China influenced greatly by the Asian Monsoons (left top: 115.0° E, 26.0°N; left  
299 bottom: 119.0° E, 24.0°N; right bottom: 124.0° E, 31.0°N; right top: 120.0° E, 34.0°N); Sub-Region 3  
300 represents the most southern region including the island Hainan in the tropical zone (left top: 105.0° E,  
301 24.0°N; right bottom: 115.0° E, 18.0°N); Sub-Region 4 represents the inner area of China covering the  
302 Yunnan-Kweichow Plateau and Sichuan Basin, under a humid inland climate (left top: 100.0° E, 33.0°N;  
303 right bottom: 107.0° E, 27.0°N); Sub-Region 5 represents the most southern Tibetan Plateau along the  
304 Himalayas with complex terrains and high elevations above ~ 4000.0 meters (left top: 80.0° E, 33.0°N;  
305 right bottom: 95.0° E, 27.0°N); Sub-Region 6 represents the central Asia with complex terrains covering  
306 the entire Tianshan Mountains in China under an arid inland climate (left top: 80.0° E, 45.0°N; right  
307 bottom: 92.0° E, 40.0°N).



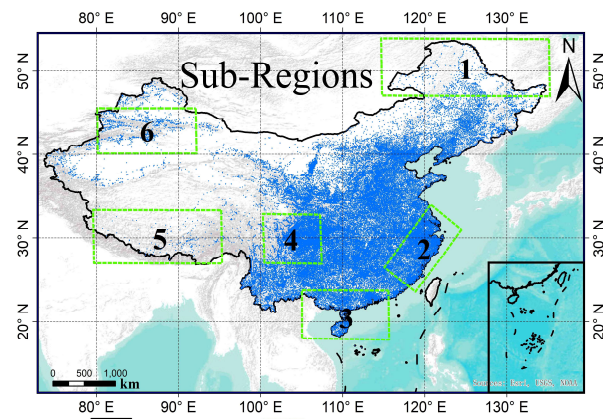
(a)



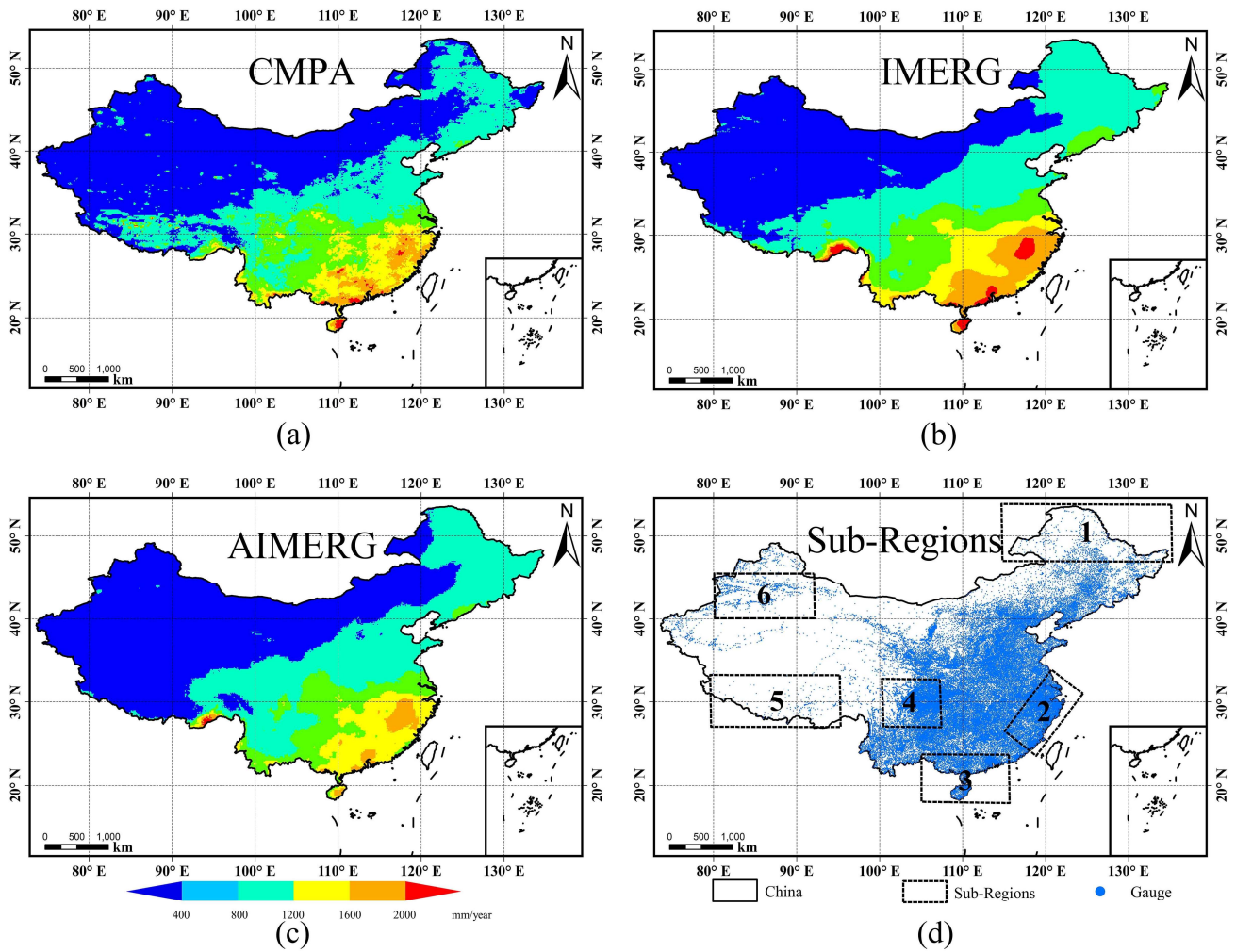
(b)



(c)



(d)



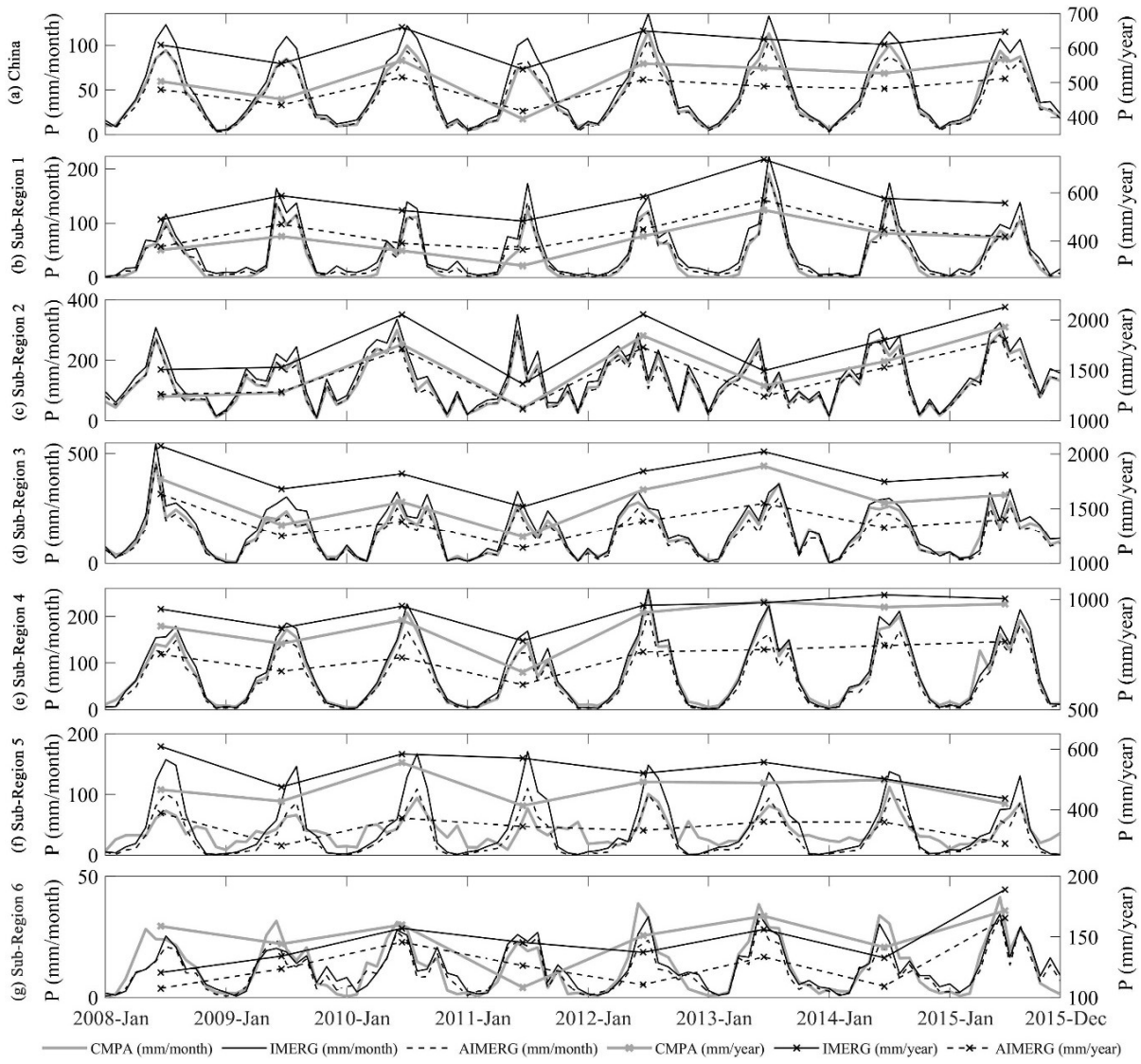
309

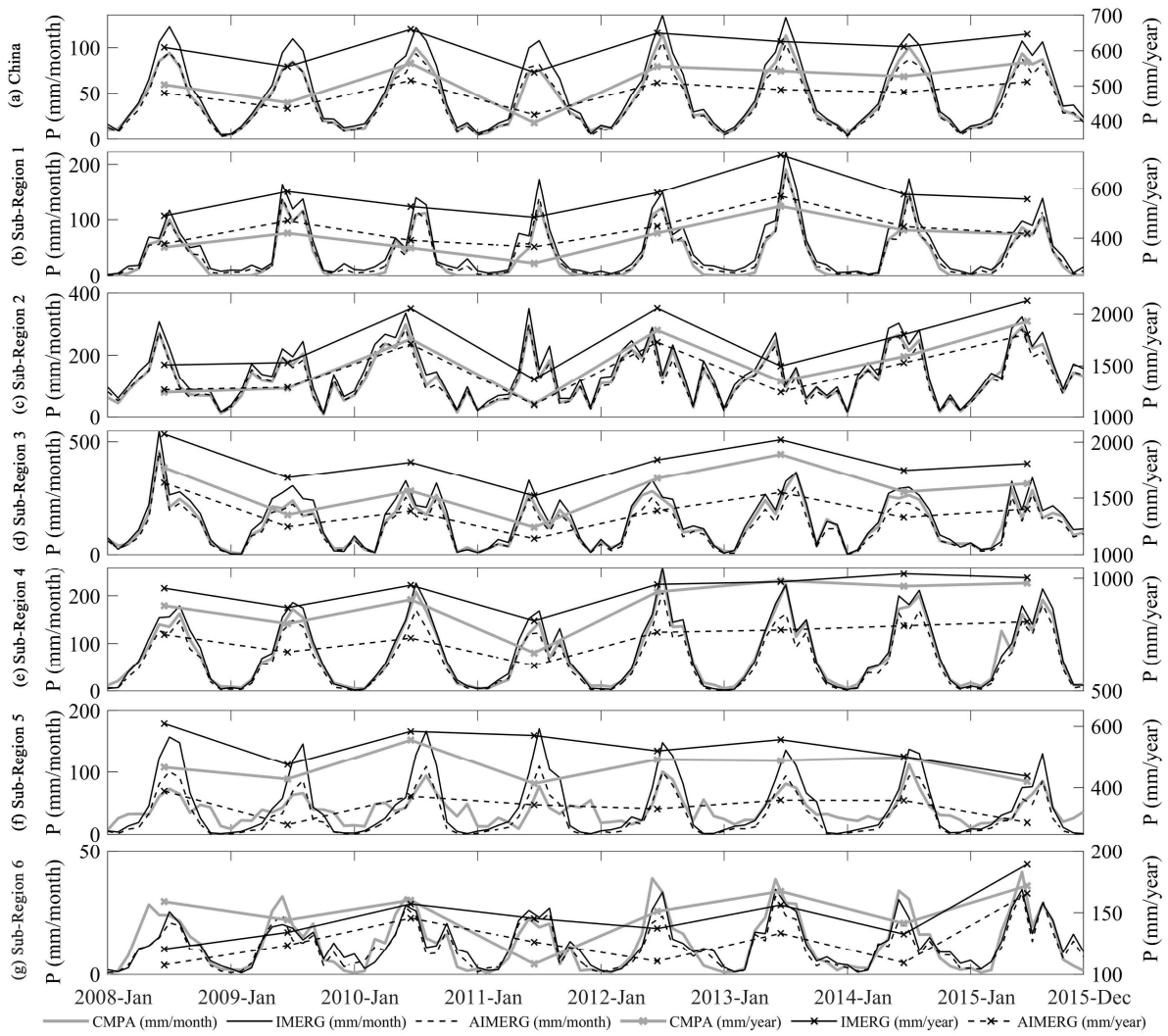
310 Figure 4 Spatial patterns of (a) CMPA, (b) IMERG, and (c) AIMERG over China Mainland From 2008~  
 311 to 2015, and (d) the spatial distributions of more than the~ 50, 000 automatic meteorological stations in  
 312 China Mainland. The accurate boundary information of the Sub-Regions: Sub-Region 1 (left top: 115.0°  
 313 E, 54.0°N; right bottom: 135.0° E, 47.0°N); Sub-Region 2 (left top: 115.0° E, 26.0°N; left bottom: 119.0°

314 E, 24.0°N; right bottom: 124.0° E, 31.0°N; right top: 120.0° E, 34.0°N); Sub-Region 3 (left top: 105.0°  
315 E, 24.0°N; right bottom: 115.0° E, 18.0°N); Sub-Region 4 (left top: 100.0° E, 33.0°N; right bottom: 107.0°  
316 E, 27.0°N); Sub-Region 5 (left top: 80.0° E, 33.0°N; right bottom: 95.0° E, 27.0°N); Sub-Region 6 (left  
317 top: 80.0° E, 45.0°N; right bottom: 92.0° E, 40.0°N). ~~The background map used in this study was provided  
318 by Esri, USGS and NOAA ([http://goto.arcgisonline.com/maps/World\\_Terrain\\_Base](http://goto.arcgisonline.com/maps/World_Terrain_Base), last access: 17  
319 January 2020).~~

320

321 The magnitudes of IMERG, AIMERG, and CMPA are compared at national and regional scale  
322 over the China Mainland from 2008 to 2015 (Fig. 5). Generally speaking, CMPA and AIMERG are almost  
323 same, and are significantly smaller than IMERG at both annual and monthly scales, additionally, CMPA  
324 is still a little larger than AIMERG over the China Mainland, which could be possibly resulted from the  
325 use of satellite observations in the CMPA and IMERG (Fig. 6a). The overall situations of the three  
326 product in sub-region 1 and 2 are similar with those over the China Mainland (Fig. 6 b-c), while both  
327 CMPA and IMERG are both significantly larger than AIMERG (Fig. 6 d-f). In sub-region 6, the Tianshan  
328 Mountains, CMPA is almost even larger than IMERG, which indicates that large uncertainties should be  
329 focused on sub-region 6 (Fig. 6 g).





331

332

Figure 5. The temporal patterns of mean areal precipitation of the IMERG, CMPA, and AIMERG, over

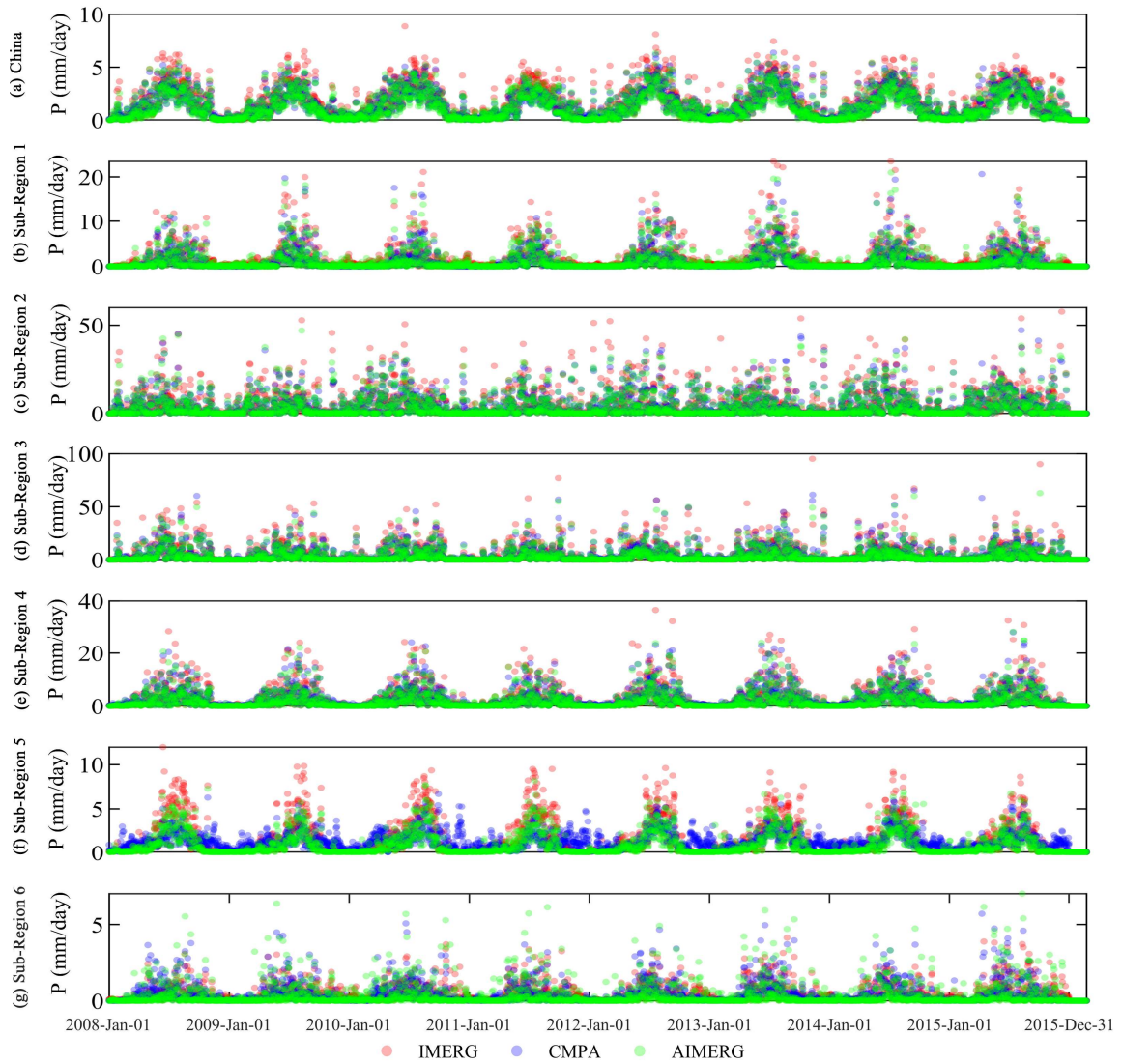
333

China Mainland and sub-regions from 2008 to 2015, at monthly and annual scales.



334 As this study aims to propose a new algorithm for calibrating the IMERG product at the daily scale,  
335 the daily spatial patterns of IMERG, CMAPA, and AIMERG ~~were~~have also been explored, which  
336 generally agree with those of IMERG, CMAPA, and AIMERG at monthly scale (Fig. 6). In mountainous  
337 region, along the Himalayas, with relatively small precipitation, CMAPA is greatly larger and smaller than  
338 the other two products (both IMERG and AIMERG) in dry seasons and wet seasons respectively (Fig. 6  
339 f). One phenomenon should be noted that the CMAPA seems abnormal along the Himalayas, which might  
340 be resulted by the limited ground observations used in CMAPA, shown in Fig. 4d, while APHRODITE  
341 data integrate large numbers of ground observations from the neighbor countries, such as India, Nepal,  
342 Bhutan, providing valuable information for retrieving high quality precipitation product around the  
343 Tibetan Plateau (Yatagai, 2012). Calibrated by APHRODITE at daily scale, AIMERG is significantly  
344 smaller than IMERG and CMAPA at both annual and monthly scale, while there are also some situations  
345 that AIMERG is larger than IMERG and CMAPA at daily scale, for example in sub-region 6, over the  
346 Tianshan mountains.

347



348

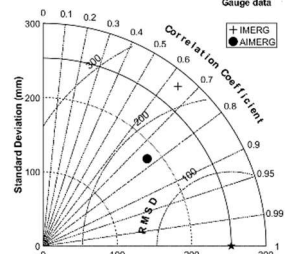
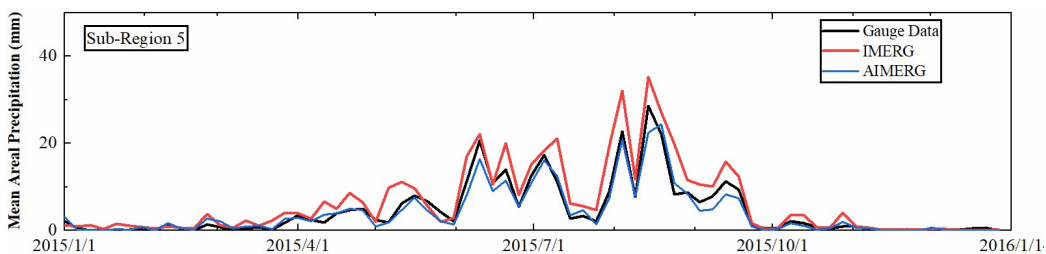
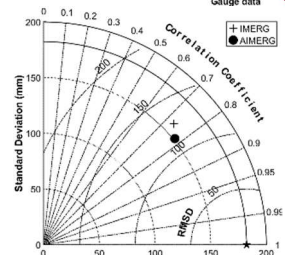
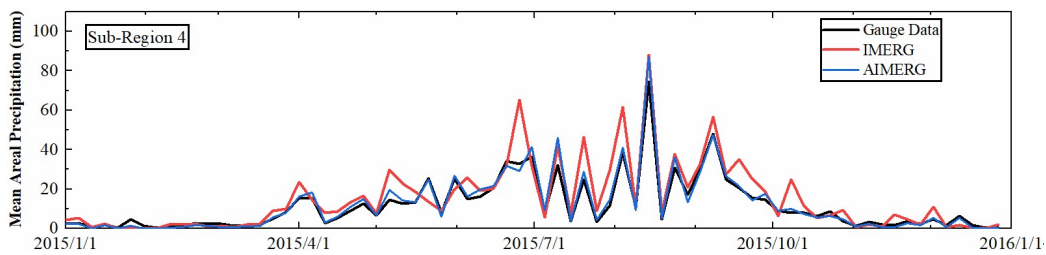
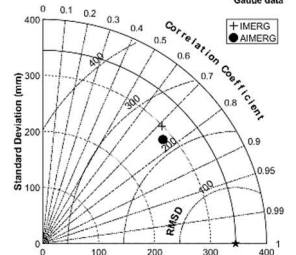
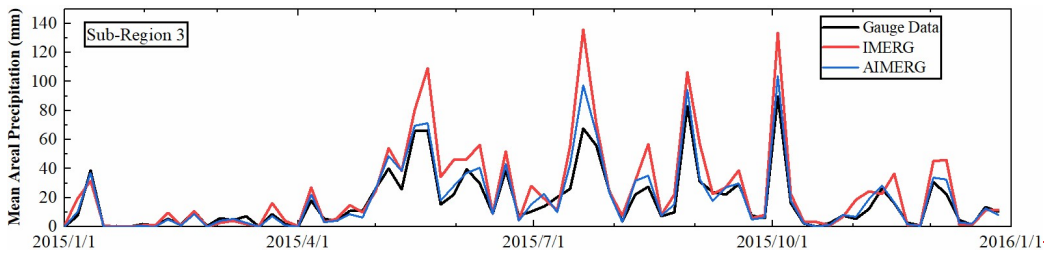
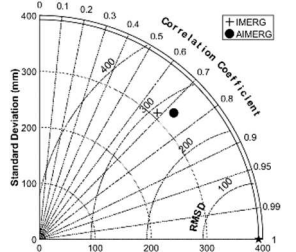
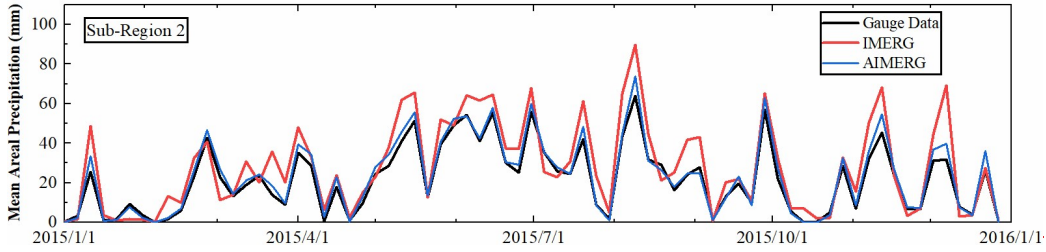
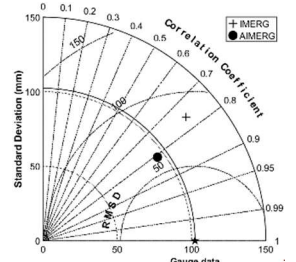
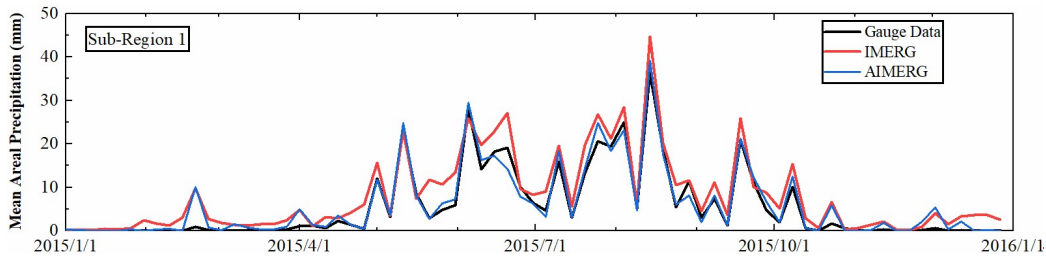
349 Figure 6. The temporal patterns of mean areal precipitation of the IMERG, CMPA, and AIMERG, over  
 350 China Mainland and sub-regions from 2008 to 2015, at daily scale.

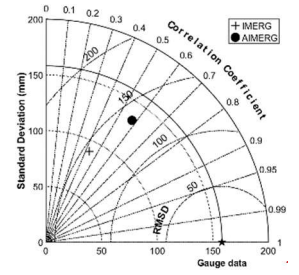
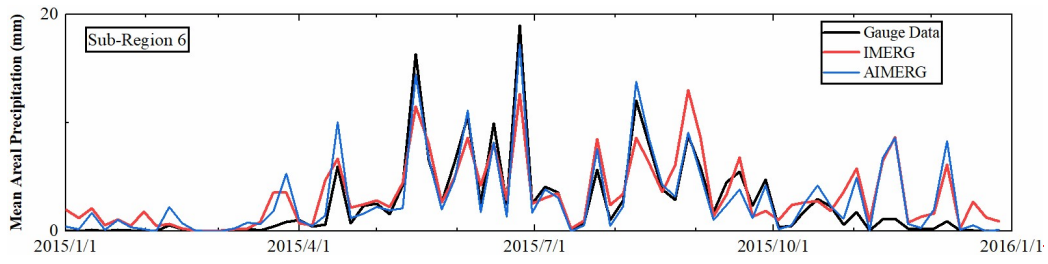
351



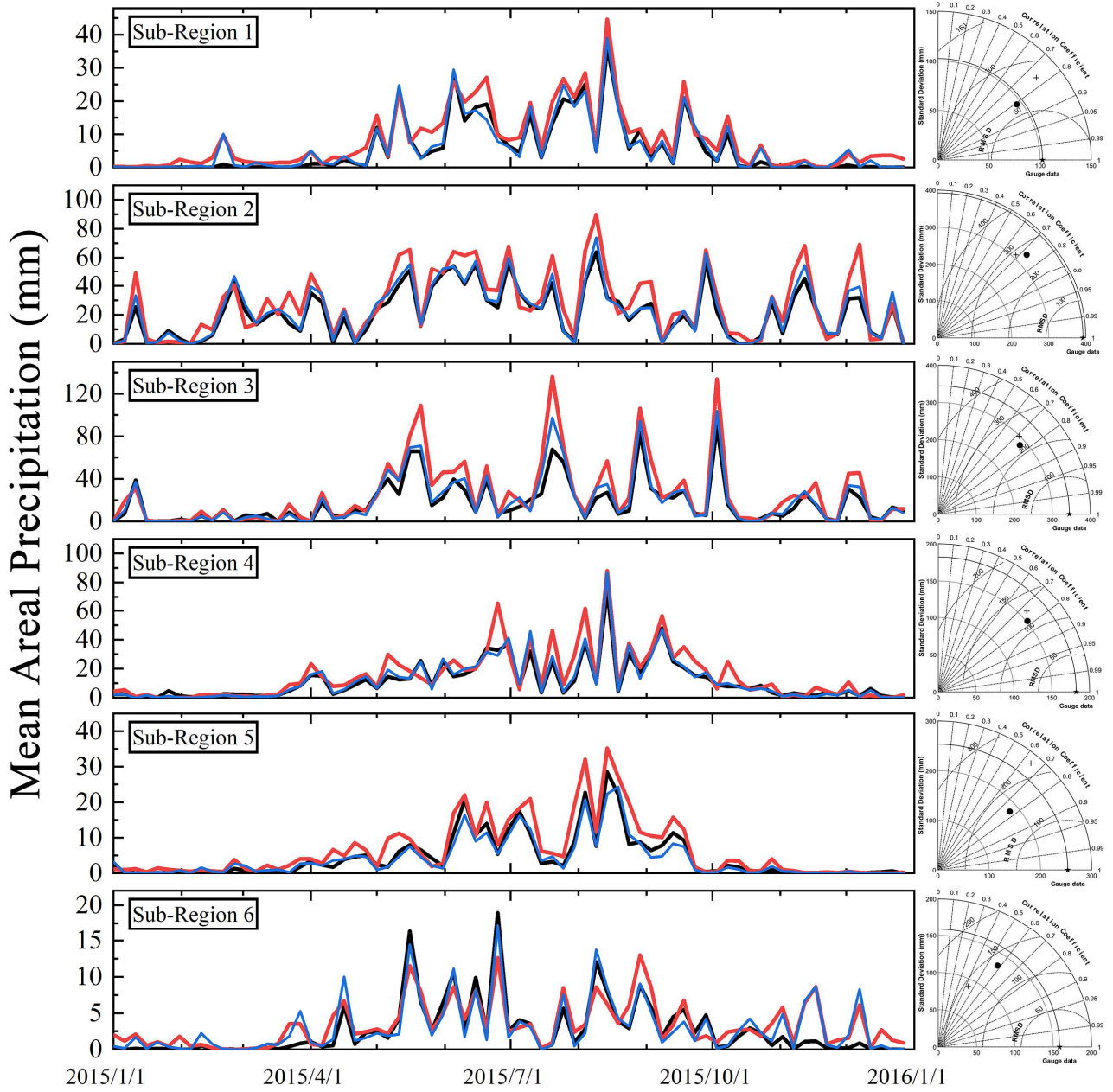
352 Hourly ground observation data from more than 50,000 meteorological stations were used to assess  
353 the quality of the IMERG and its calibrations, AIMERG, over the six sub-regions, in 2015 (Fig. 7). The  
354 temporal patterns and volumes of mean areal precipitation by AIMERG and ground observations are  
355 almost same, while IMERG is generally larger than AIMERG and ground observations. Meanwhile, the  
356 IMERG still has the problems in overestimating and underestimating the precipitation in dry seasons  
357 (relatively large precipitation occurring) and wet seasons (relatively small precipitation happening),  
358 respectively, for example in sub-region 6, over the Tianshan Mountains. In terms of quantitative indices  
359 (Standard deviation, RMSD, and CC), AIMERG generally outperforms the IMERG against the ground  
360 observations, especially in sub-region 5, along the Himalayas, which indicates that the ground information  
361 from the neighbor countries integrated into the APHRODITE data greatly benefits the calibration results,  
362 AIMERG.

363





— Gauge Data    — IMERG    — AIMERG    + IMERG    ● AIMERG

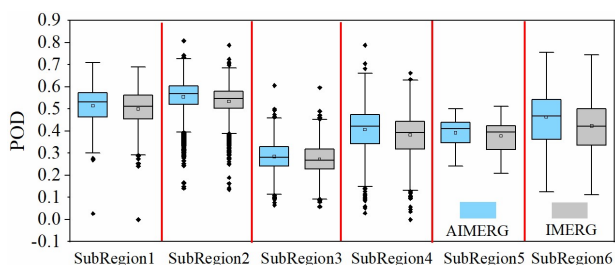


364

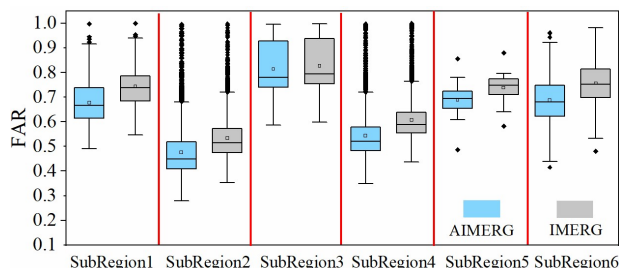
365 Figure 7. The temporal patterns and the volumes of IMERG, ground observations, and AIMERG, in six  
366 sub-regions at daily scale; and the Taylor diagrams of performances on IMERG and AIMERG against  
367 ground observations in terms of centered root-mean-square difference, correlation coefficient and  
368 standard deviation in the six sub-regions at hourly scale, in 2015.

369

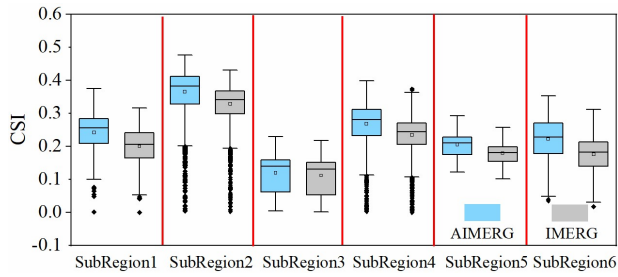
370 Figure 8 illustrates the numerical distributions of contingency statistics for IMERG and AIMERG,  
371 at hourly scale, in six sub-regions, 2015. Generally, the POD values of AIMERG are larger than those of  
372 IMERG (Fig. 8a), and FAR values of AIMERG are overall smaller than those of IMERG in each sub-  
373 regions (Fig. 8b), which results the better performances of the comprehensive index, CSI, combining both  
374 the characteristics of POD and FAR, in each sub-regions (Fig. 8c). Additionally, both the IMERG and  
375 AIMERG perform best in sub-region 2, and worst in sub-region 3.



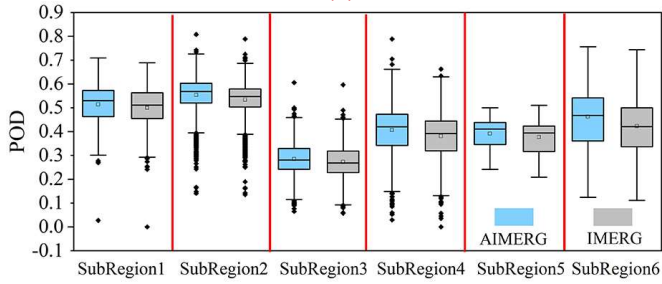
(a)



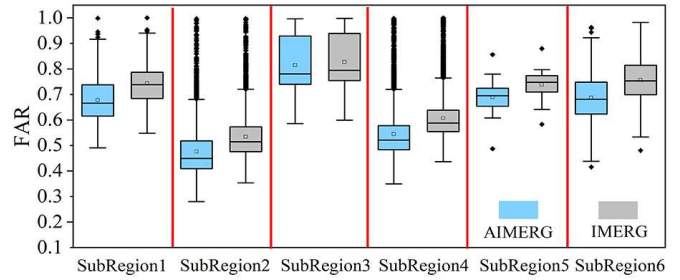
(b)



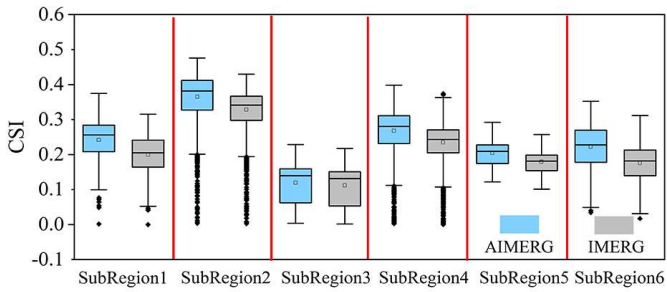
(e)



(a)



(b)



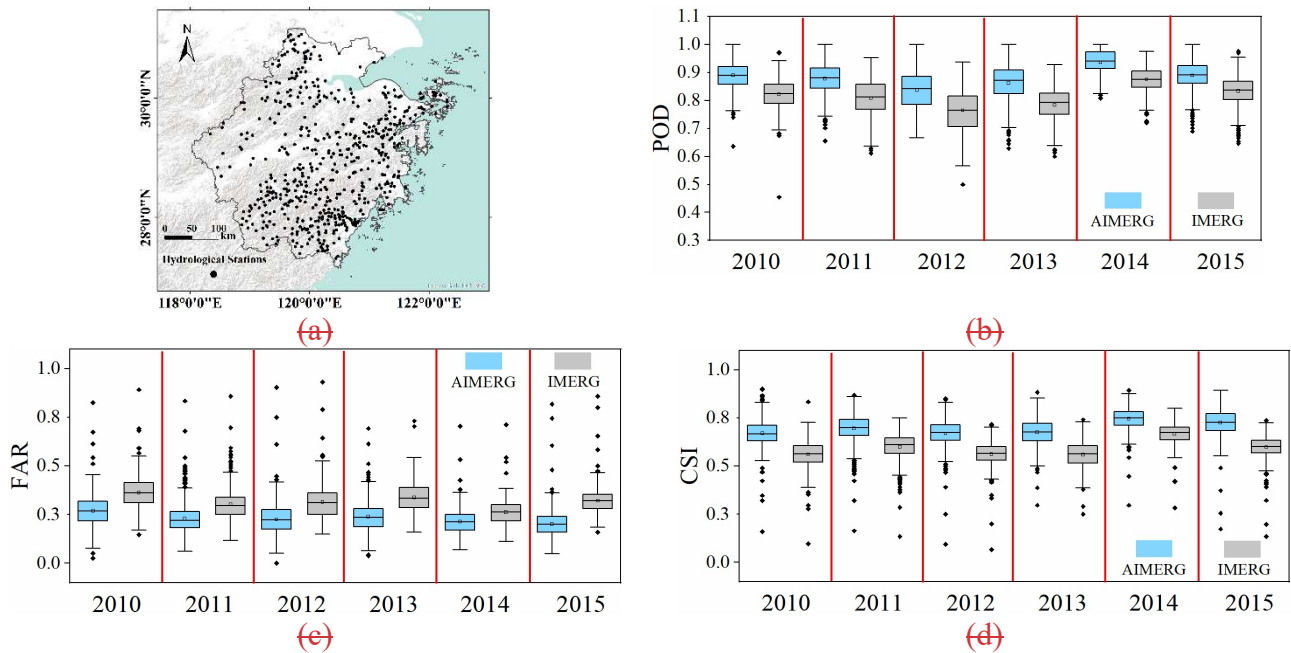
(c)

376

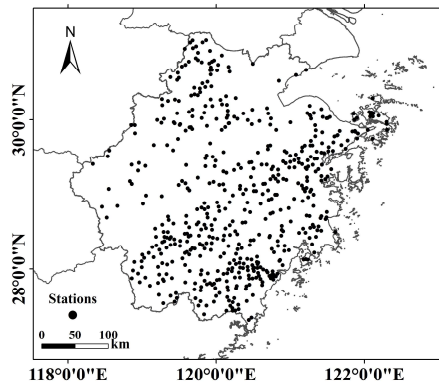
377 Figure 8. The boxplots demonstrate diagnose of IMERG and AIMERG against the ground observations  
 378 from the meteorological stations, at hourly scale, in six sub-regions, 2015.

379

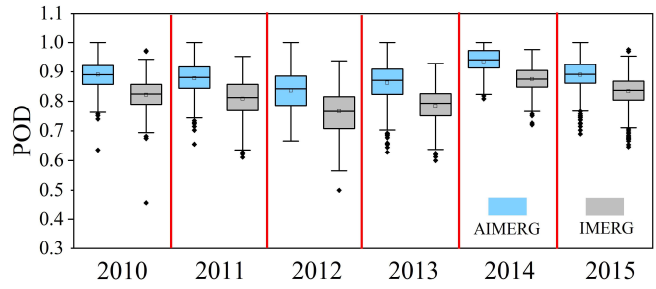
380 To assess the quality of the IMERG and AIMERG, entirely independent precipitation data from  
 381 around 500 hydrological stations, at hourly scale, from 2010 to 2015, were applied, which are relatively  
 382 even distributed in Zhejiang province (Fig. 9a). The POD values of AIMERG ( $\sim 0.9$ ) are general larger  
 383 than those of IMERG ( $\sim 0.8$ ), while the FAR values of AIMERG ( $\sim 0.3$ ) are significantly smaller than  
 384 those of IMERG ( $\sim 0.4$ ), which results in the overall capabilities of AIMERG to capture the precipitation  
 385 events are improved more than 10%, compared with IMERG, in terms of the CSI. The relative smaller  
 386 POD values and larger FAR values of IMERG in the Zhejiang province, southeastern coast of China,  
 387 might be one of the potential drawbacks in accurately estimating the precipitation both qualitatively and  
 388 quantitatively.



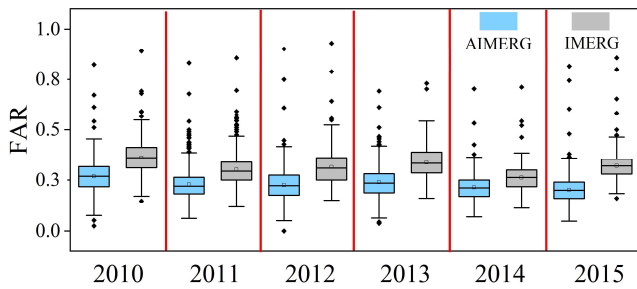




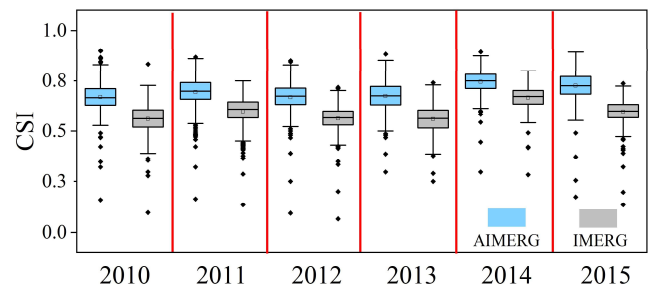
(a)



(b)



(c)



(d)

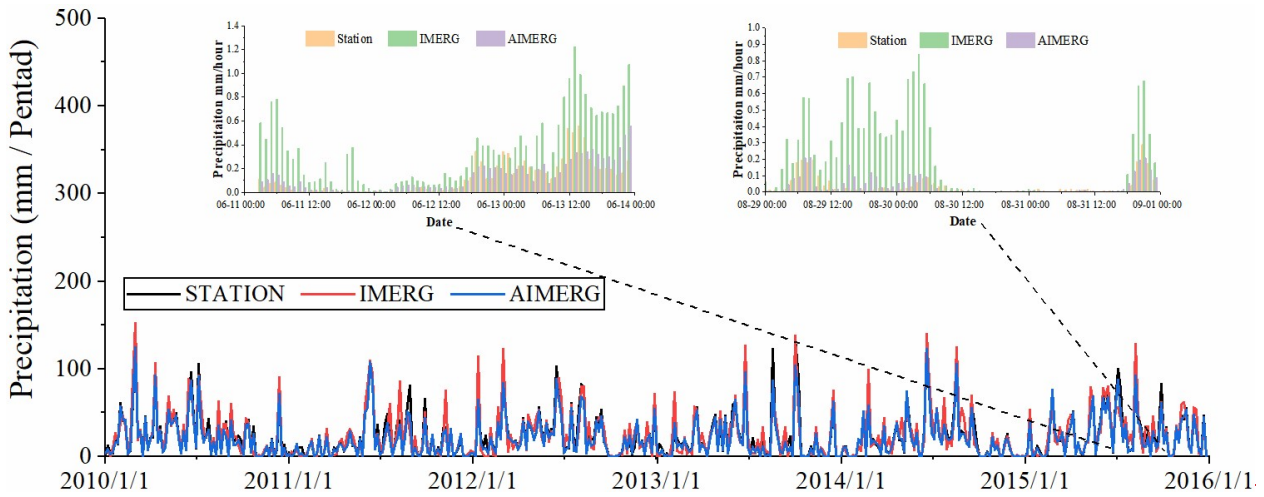
389

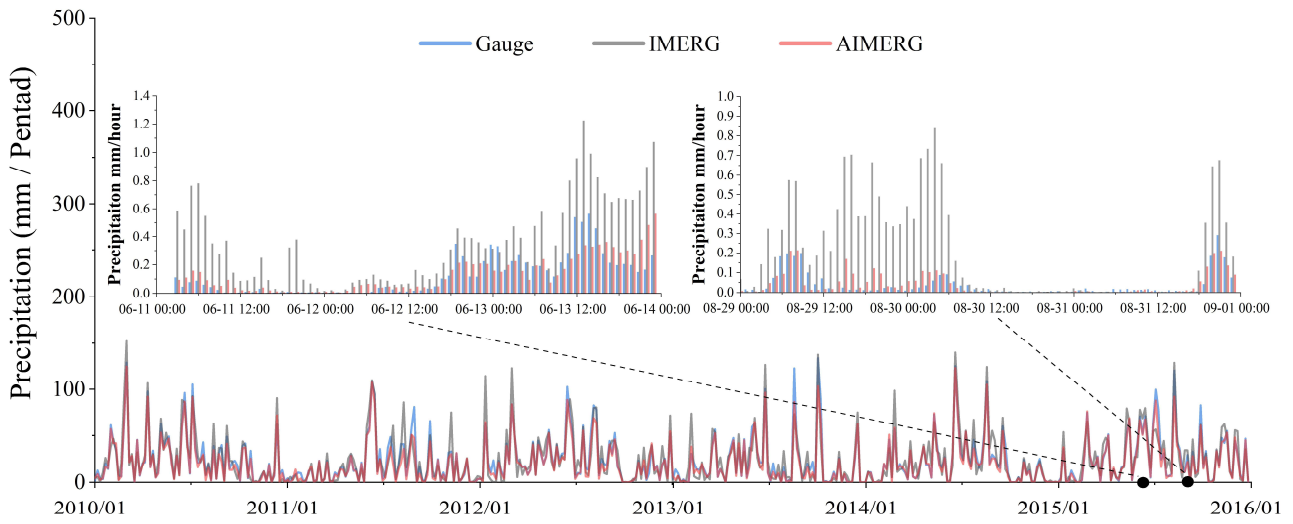
390 Figure 9. The boxplots demonstrate diagnose of IMERG and AIMERG against the ground observations  
 391 from hydrological stations, respectively, at hourly scale, in Zhejiang province, 2010-2015. ~~The~~  
 392 ~~background map used in this study was provided by Esri, USGS and NOAA~~  
 393 ~~([http://goto.arcgisonline.com/maps/World\\_Terrain\\_Base](http://goto.arcgisonline.com/maps/World_Terrain_Base), last access: 17 January 2020).~~

394 From the temporal patterns of mean areal precipitation of IMERG, AIMERG, and ground  
 395 observations from hydrological stations, in Zhejiang province, 2010-2015 (Fig. 10), IMERG is general  
 396 larger than both AIMERG and ground observations. For instance, the IMERG significantly overestimates



397 the precipitation with up to ten times than that of AIMERG and ground observations, such as in the typical  
398 periods, 0 a.m., June, 11 – 0 a.m., June, 14, 2015, and 0 a.m., Aug, 29 – 0 a.m., Sep, 1, 2015. Additionally,  
399 both the temporal patterns and the magnitudes of AIMERG are almost same with those of ground  
400 observations, compared with those of IMERG. Meanwhile, in some pentads with the heavy rain events,  
401 both AIMERG and ground observations are larger than IMERG.





403

404

405

406

Figure 10. The temporal patterns of mean areal precipitation of IMERG, AIMERG, and the ground observations from the independent hydrological stations, at daily/hourly scale, in Zhejiang province, 2010-2015.

407

### 4.3. The performances of AIMERG and other products in capturing the heavy rainfall event

408

409

410

411

412

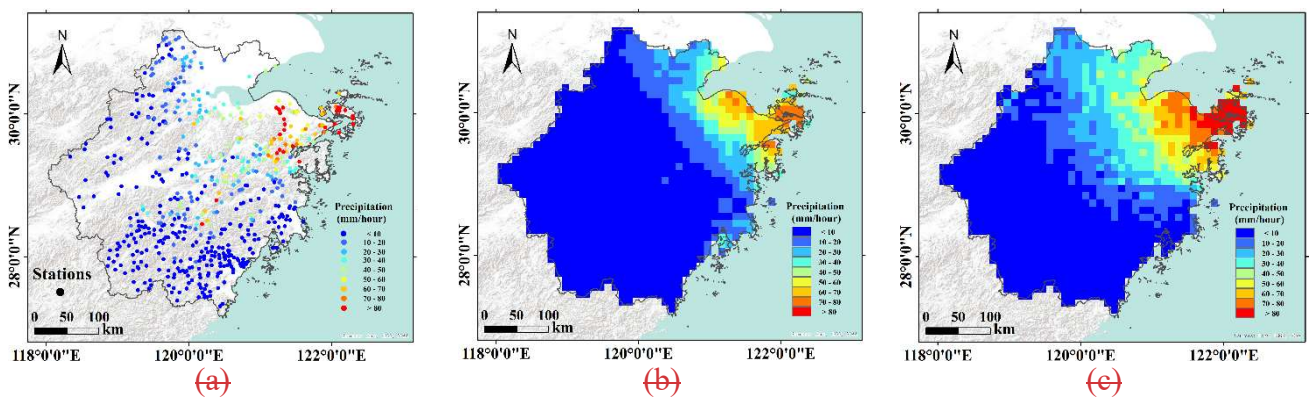
413

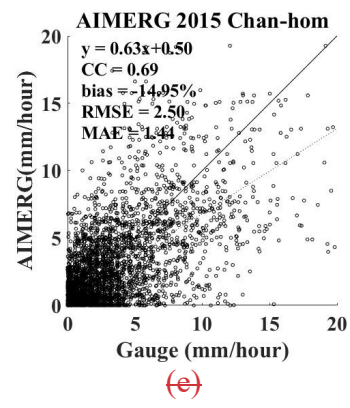
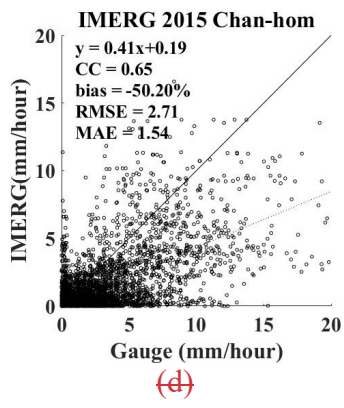
One of the primary aims of the satellite-based precipitation estimates is to provide the high quality rainfall information, accurately capturing both the spatial patterns and volumes of the rainfall, at hourly scale during the heavy rainfall events. Recently, Tang et al (2020) has conducted a comprehensive comparison of GPM IMERG with other nine state-of-the-art high resolution precipitation products, six satellite-based precipitation products (TRMM 3B42, 0.25°/3 hour; CMORPH, 0.25°/3 hour; PERSIANN-CDR, 0.25°/1 day; GSMaP 0.1°/1 hour; CHIRPS, 0.05°/1 day; SM2RAIN, 0.25°/1 day) and three

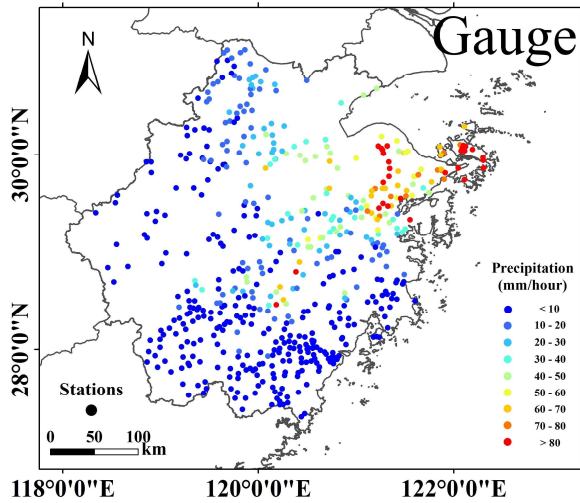
414 reanalysis datasets (ERA5,  $\sim 0.25^\circ/1$  hour; ERA-Interim,  $\sim 0.75^\circ/3$  hour; MERRA2  $\sim 0.5^\circ \times 0.625^\circ/1$  hour)  
415 from 2000 to 2018, and found that the IMERG product generally outperformed other datasets, except the  
416 Global Satellite Mapping of Precipitation (GSMaP), which was adjusted at the daily scale by the gauge  
417 analysis ( $0.5^\circ/\text{daily}$ ) from the CPC (Mega et al., 2014). Therefore, we have quantitatively and horizontally  
418 compared the AIMERG with GSMaP, as well as the IMERG against ground observations.

419 In this study, the typhoon, Chan-hom, is selected as an example for assessing the quality of  
420 AIMERG and other products, occurred in the typical period 0 a.m., – 11 a.m., July, 11, 2015, in Zhejiang  
421 province (Fig. 11 a-d). Generally, the spatial patterns of the IMERG, GSMaP, AIMERG are similar with  
422 those of the ground observations, with the increasing volumes of rainfall from southwest to northeast. In  
423 terms of the three satellite-based rainfall estimates, IMERG underestimates the rainfall greater than those  
424 of GSMaP and AIMERG, in the heavy rainfall events (Fig. 11 b), with largest regions in the southwestern  
425 Zhejiang (rainfall  $< 10$  mm/hour). Though GSMaP estimates the rainfall greater than IMERG in both  
426 spatial coverages and volumes (Fig. 11 c), the AIMERG provides much more details than GSMaP,  
427 especially over the northeastern Zhejiang Province (Fig. 11 c). As pointed out by various studies (e.g.,  
428 Tang et al., 2020), the satellite-based precipitation products generally overestimate the volumes in small  
429 rainfall events, but underestimate the volumes during the heavy rainfall events. From this aspect,  
430 AIMERG outperforms the GSMaP as well as the original IMERG, owing to the daily calibrations using  
431 the ground observations.

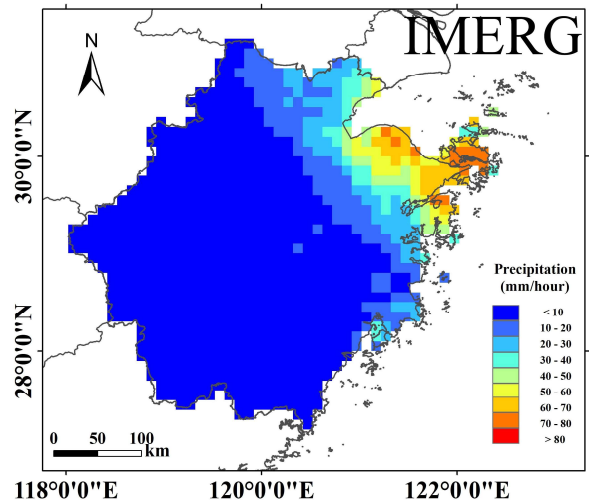
432 One of the primary aims of the satellite-based precipitation estimates is to provide the high quality  
 433 precipitation information at hourly scale in the heavy rainfall events. Therefore, one typhoon event, Chan-  
 434 hom, is selected as an example for assessing the quality of the IMERG and AIMER in Zhejiang Province,  
 435 where is always threatened by the typhoons, shown in Fig. 11. Though the spatial patterns of IMERG and  
 436 AIMERG are both similar to those of ground observations, IMERG still underestimates the precipitation,  
 437 compared with AIMERG (Fig. 11 a-c). From the statistics, not only the systematic bias of IMERG (around  
 438 -50%) is significantly improved, with bias of AIMERG around -10%, but also the random errors of  
 439 IMERG (RMSE  $\sim$  2.7 mm/hour, MAE  $\sim$  1.5 mm/hour) are also reduced, compared with AIMERG (RMSE  
 440  $\sim$  2.5 mm/hour, MAE  $\sim$  1.4 mm/hour), which meant the calibrations using APHRODITE on IMERG  
 441 improved the abilities of original IMERG product to more accurately estimate the quantitative  
 442 precipitation volumes, especially in heavy rainfall events (Fig. 11 e-d).



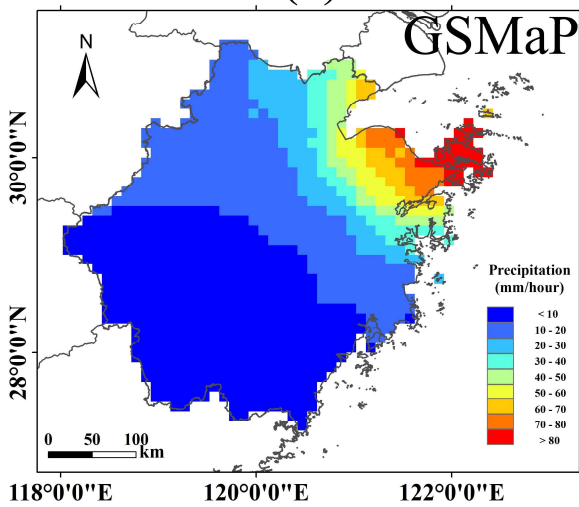




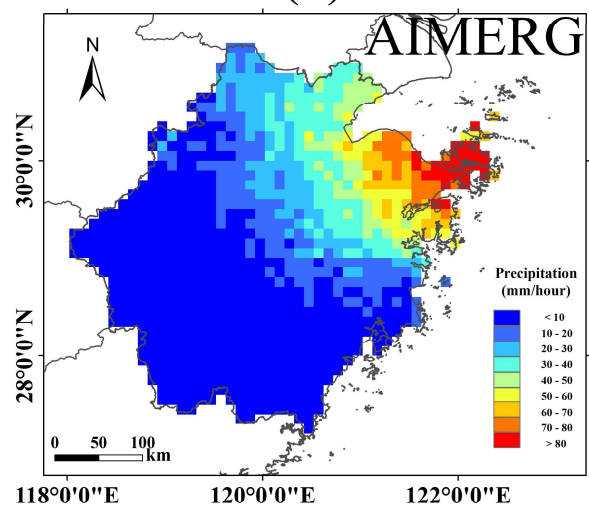
(a)



(b)



(c)



(d)

443

444

445

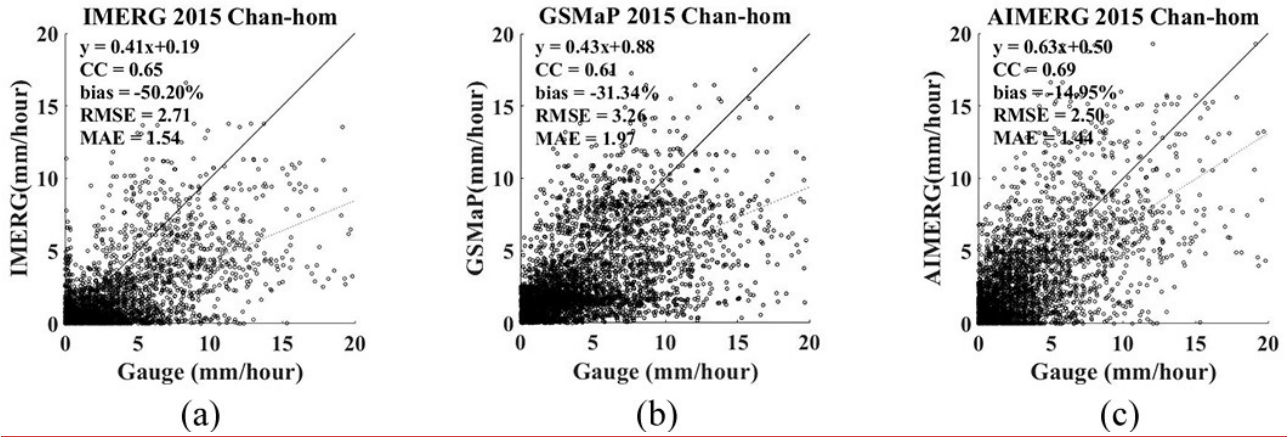
Figure 11. The spatial patterns of precipitation measured by (a) IMERG, (b) GSMaP, and (c) AIMERG, during The typhoon, Chan-hom, is selected as an example for assessing the quality of the IMERG and

446 ~~AIMER~~, occurred in the typical period 0 a.m., – 11 a.m., July, 11, 2015, in Zhejiang Province. ~~The~~  
447 ~~background map used in this study was provided by Esri, USGS and NOAA~~  
448 ~~([http://goto.arcgisonline.com/maps/World\\_Terrain\\_Base](http://goto.arcgisonline.com/maps/World_Terrain_Base), last access: 17 January 2020).~~

449  
450 To quantitatively assess the performances of the AIMERG, GSMaP, and IMERG, they are also  
451 evaluated against the ground observations, during the typhoon, Chan-hom, occurred in the typical period  
452 0 a.m., – 11 a.m., July, 11, 2015, in Zhejiang province (Fig. 12 a-c). From the statistics, not only the  
453 systematic bias of IMERG (around -50%) is significantly improved, with the bias of AIMERG around -  
454 10%, but also the random errors of IMERG (RMSE ~ 2.7 mm/hour, MAE ~ 1.5 mm/hour) are also reduced,  
455 compared with AIMERG (RMSE ~ 2.5 mm/hour, MAE ~ 1.4 mm/hour), which meant the calibrations  
456 using APHRODITE on IMERG improved the abilities of original IMERG product to more accurately  
457 estimate the quantitative precipitation volumes, especially in heavy rainfall events (Fig. 12 a and c).  
458 Meanwhile, AIMERG significantly overwhelms GSMaP in terms of both bias and random errors. For  
459 instance, GSMaP underestimates the precipitation (bias ~ -31%) twice as large as AIMERG (bias ~ -15%),  
460 and the random errors of GSMaP (MAE ~ 1.97 mm/hour, RMSE ~ 3.26 mm/hour) are also significantly  
461 larger than those of AIMERG (MAE ~ 1.44 mm/hour, RMSE ~ 2.50 mm/hour) (Fig. 12 b and c).  
462 Compared with the original IMERG, though the random errors of GSMaP are relatively larger, the bias  
463 of GSMaP (~ -31%) is significantly smaller than that of the original IMERG (~ -50%), which owes to the



464 calibrations on the GSMaP at the daily scale (Fig. 12 a and b). In future, we also encourage researchers  
465 to comprehensively evaluate and compare the AIMERG with other high resolution precipitation products  
466 at various spatio-temporal scales.



468 Figure 12. The scatterplots of (a) IMERG, (b) GSMaP, and (c) AIMERG against ground observations  
469 during the typhoon, Chan-hom, occurred in the typical period 0 a.m., – 11 a.m., July, 11, 2015, in Zhejiang  
470 Province.

471 The extent of the AIMERG could cover the Northern Eurasia, Middle East, Monsoon Asia, and  
472 Japan. This study mainly evaluated the AIMERG in the China Mainland, which calls for Asia wide  
473 evaluations in the future to assess both the algorithm and the corresponding precipitation product. For  
474 regions with relative dense rain gauge networks, it is better to quantitatively and horizontally evaluate  
475 the AIMERG and other precipitation estimates against ground observations, using statistical evaluations  
476 (Lu et al., 201; Xu et al., 2019; Tang et al., 2020), for example, in Japan, and Monsoon India. While for



477 regions with relative sparse rain gauge networks, it is optimal to horizontally compare the performances  
478 and abilities of AIMERG with those of other products in precipitation-related application fields, e.g., in  
479 hydrological simulations at basin scales (Ma et al., 2018).

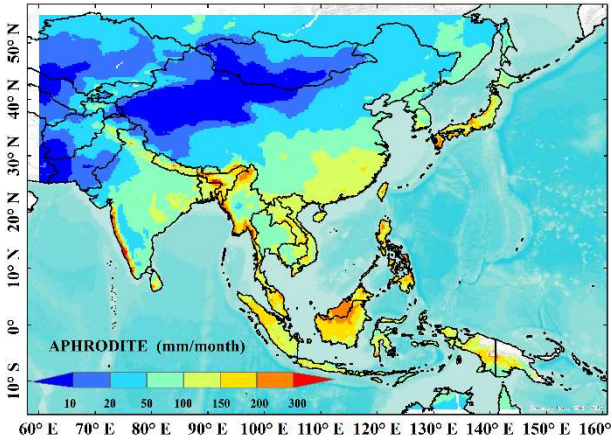
## 481 **5. Discussions**

### 482 **5.1. The potential drawbacks in processing the IMERG product**

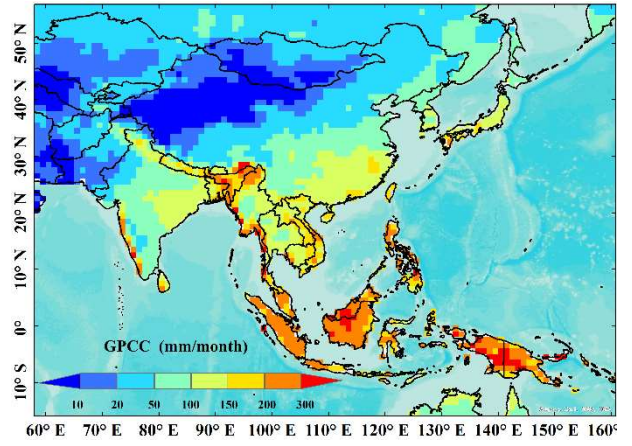
483 From the document of “Algorithm Theoretical Basis Document (ATBD) Version 06” for  
484 generating the final IMERG product (Huffman et al., 2019a), we find that there are mainly two steps in  
485 the process: the first step is to derive the multi-satellite-only precipitation inversion estimates, and the  
486 second step is to calibrate the ~~multi-satellite-only~~ satellite-based-only precipitation estimates using the  
487 interpolated precipitation product based on ground observations, e.g., GPCC (1.0°/monthly). As lacking  
488 mature calibration algorithm for calibrating the multi-satellite-only precipitation estimates at daily scale,  
489 the current IMERG-Final product are only calibrated using the GPCC at monthly scale. The two aims of  
490 this study are to provide (1) ~~provide~~ a spatio-temporal calibration algorithm (DSTDCA) for anchoring the  
491 satellite-based precipitation estimates at daily scale, and (2) a new precipitation product with finer quality,  
492 namely AIMERG (half-hourly,  $0.1^\circ \times 0.1^\circ$ , 2000-2015, Asia) (Ma et al., 2020a, b), for Asian researcher.  
493 For anchoring the IMERG final product, we introduce the APHRODITE data (daily,  $0.25^\circ \times 0.25^\circ$ , 2000-  
494 2015, Asia), which were interpolated based on the ground observations from the large numbers of rain

495 gauges. Though the general spatial patterns of monthly mean precipitation estimates from both  
496 APHRODITE and GPCC, from 1951 to 2015, are similar, the volumes of them demonstrate significant  
497 differences, especially along the Himalayas, coastal Indochina and Western Ghats, and the Indonesia (Fig.  
498 ~~12-13~~ a-b). To much more clearly demonstrate the relative values of GPCC and APHRODITE, the spatial  
499 patterns of the ratio of monthly mean values of APHRODITE to those of GPCC are illustrated in Fig. ~~12~~  
500 13 c, from which we find that GPCC significantly overestimates the precipitation in the tropical rain range  
501 along the Indonesia, and along the southern Himalayas with complex terrain, while it significantly  
502 underestimates the precipitation in the north western Tibetan Plateau and Middle East, compared with the  
503 ground “truth” product, APHRODITE. Illustrated by Fig. ~~12~~13, the GPCC plays vital roles ~~for~~in the final  
504 IMERG product, and the introduction of APHRODITE on calibrating the IMERG would be greatly  
505 benefiting the quality of the AIMERG.

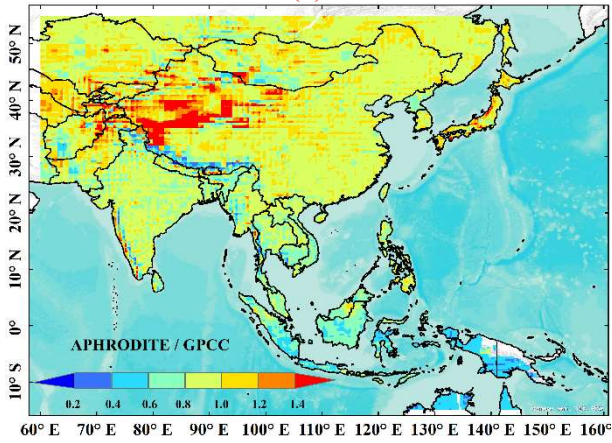
506



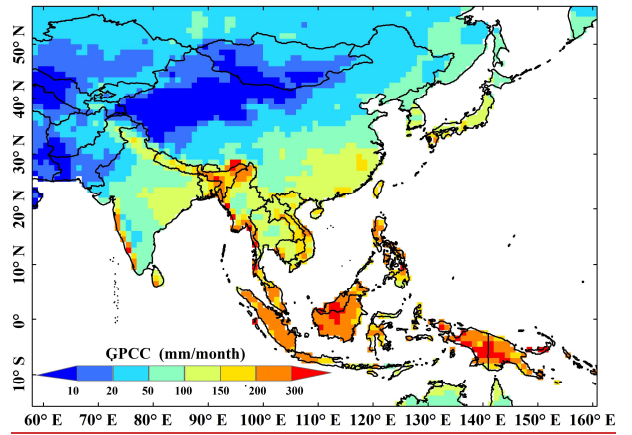
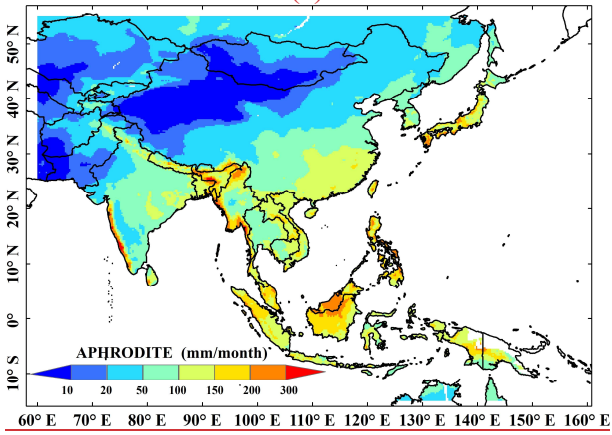
(a)

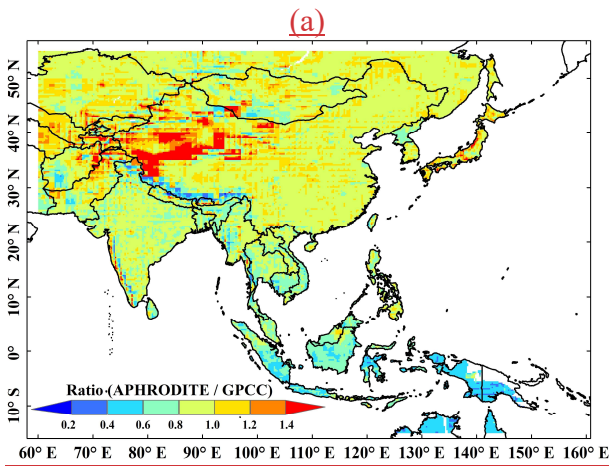


(b)



(c)



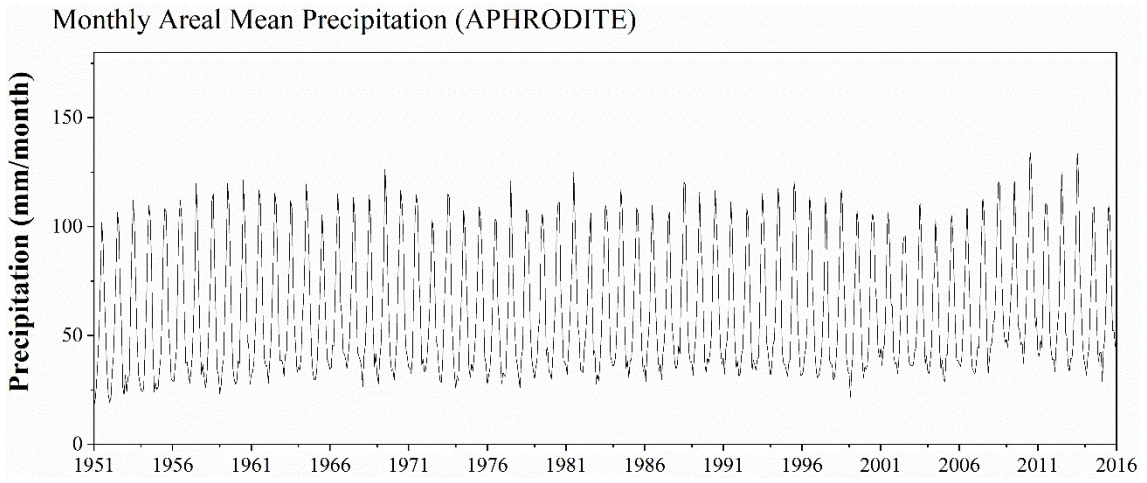


507 Figure 1213. The spatial patterns of the monthly mean precipitation of (a) APHRODITE and (b) GPCC,  
 508 and (c) Ratios between monthly mean values of APHRODITE and GPCC, over the Asia in the period  
 509 from 1951 to 2015. ~~The background map used in this study was provided by Esri, USGS and NOAA~~  
 510 ~~([http://goto.arcgisonline.com/maps/World\\_Terrain\\_Base](http://goto.arcgisonline.com/maps/World_Terrain_Base), last access: 17 January 2020).~~

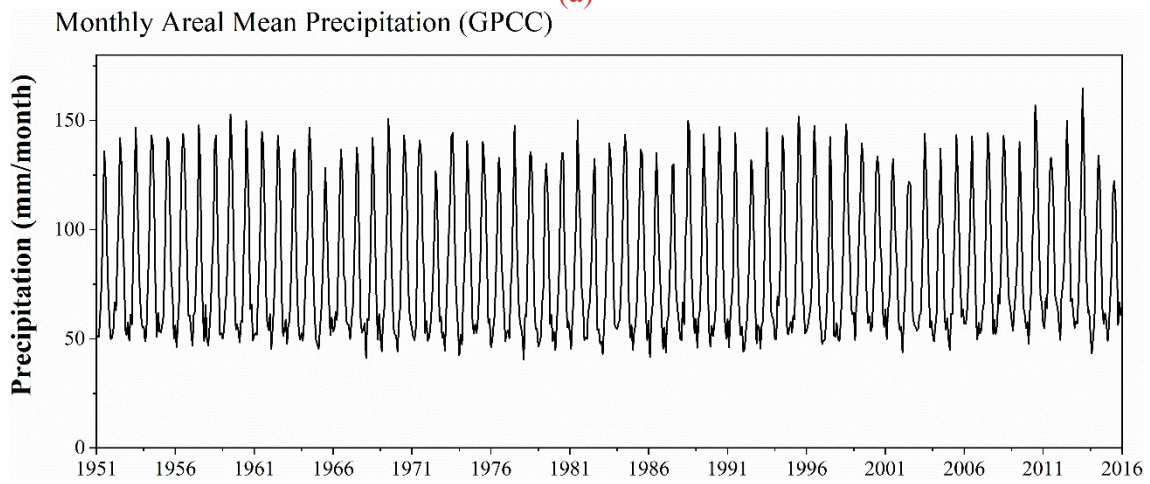
511 There are mainly two kinds of errors in the multi-satellite-only precipitation product, including  
 512 systematic bias and random errors (Shen et al., 2014). As seen in the above-mentioned results, the random  
 513 errors of the AIMERG are alleviated by using the APHRODITE data compared with IMERG (e.g., Fig.  
 514 4-1113). In terms of the systematic errors, we compared the monthly Asian mean precipitation estimates  
 515 of both APHRODITE and GPCC, from 1951 to 2015 (Fig. 1314). The monthly Asian mean precipitation  
 516 of APHRODITE varies between  $\sim 25$  mm/month and  $\sim 100$  mm/month, while those of GPCC ranges  
 517 from  $\sim 50$  mm/month and  $\sim 150$  mm/month, which results the ratios of APHRODITE to GPCC fluctuate  
 518 significantly from  $\sim 0.2$  to  $\sim 0.9$ , with average value  $\sim 0.7$ , which means that the GPCC at least

519 overestimates the precipitation more than  $\sim 30\%$ , compared with the APHRODITE. Therefore, the  
520 introduction of APHRODITE data would greatly reduce the systematic errors of the IMERG final product,  
521 over the Asia.

522

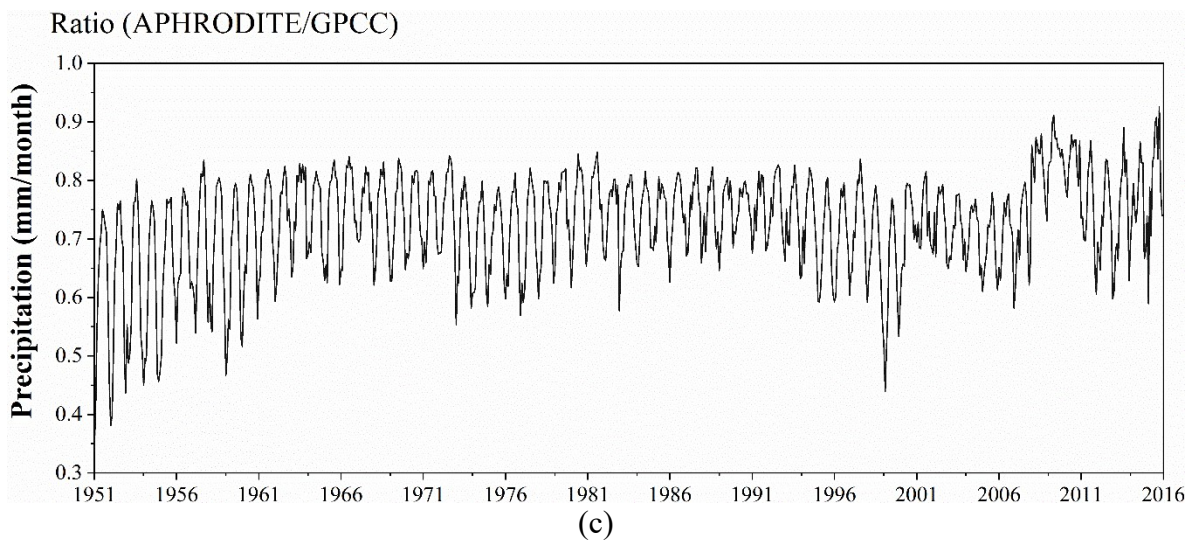


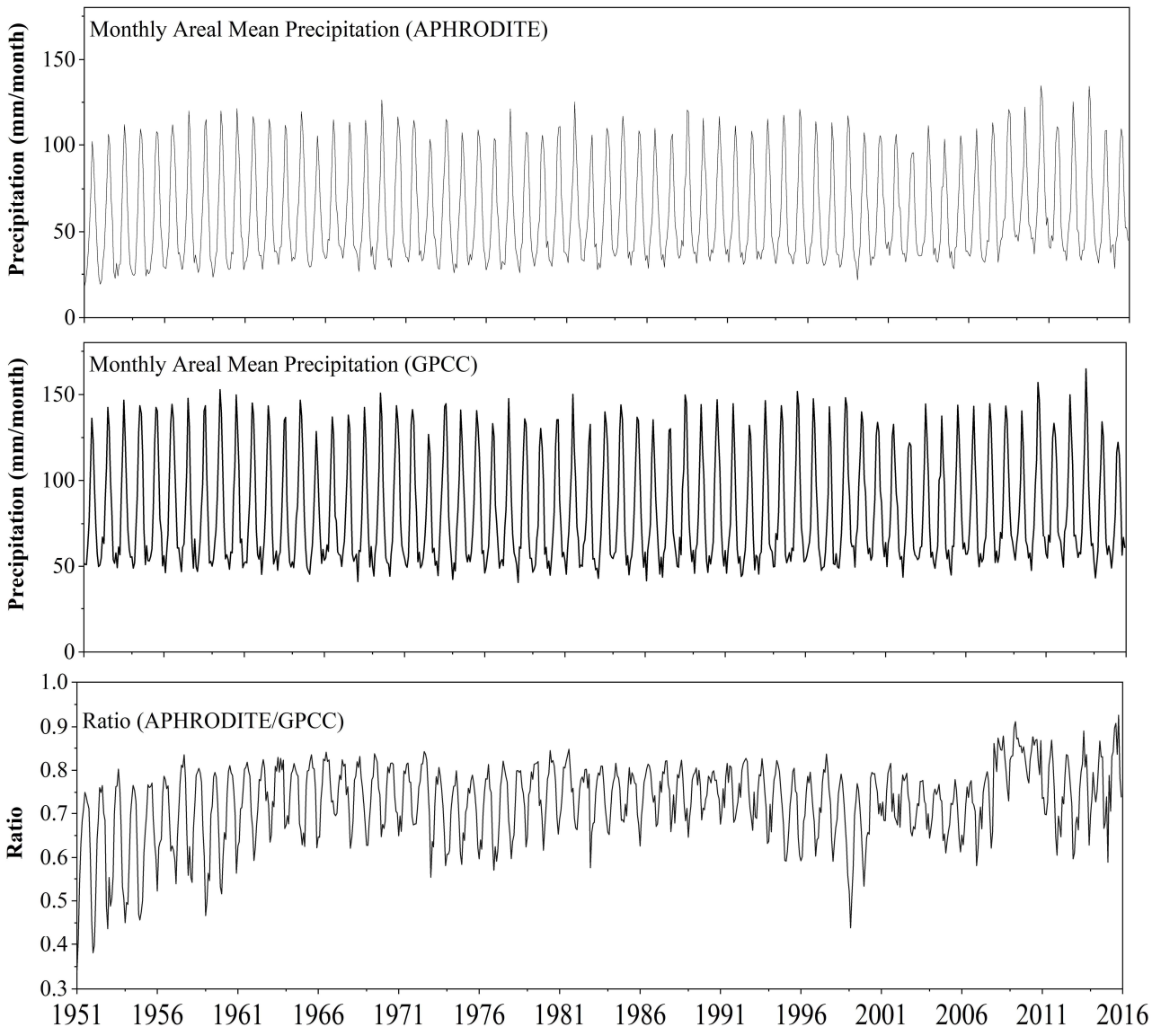
(a)



(b)







523

524

525

Figure 13.14. The temporal patterns of monthly areal mean precipitation of (a) APHRODITE, (b) GPCC, and (c) APHRODITE/GPCC, 1951-2015. The temporal patterns of monthly areal mean



526 precipitation of (a) APHRODITE and (b) GPCC, and monthly (c) ratio values of corresponding areal  
527 mean APHRODITE/GPCC, 1951-2015.

## 529 **5.2. The controls on the range of the spatial weights based on IMERG**

530 As demonstrated in the document of the “ATBD” ([Huffman et al., 2019a](#)), gauge information is  
531 introduced into the original multi-satellite-only half-hourly data to generate the final IMERG product.  
532 Firstly, the ratio between the monthly accumulation of half-hourly multi-satellite-only field and the  
533 monthly satellite-gauge field is calculated, then each half-hourly field of multi-satellite-only precipitation  
534 estimates in the corresponding month is multiplied by the ratio field to generate the half-hourly calibrated  
535 IMERG. After various experiments, the ratio values between the monthly satellite-gauge and the monthly  
536 accumulation of half-hourly multi-satellite-only fields is limited to the range [0.2, 3] (Huffman et al.,  
537 2019a). The cap of 3 is decided due to the value of 2 (used in TRMM V6) was too restrictive.  
538 Additionally Meanwhile, the cap of 3 ~~was~~ is finally applied because it performed better in matching the  
539 two accumulations than that of other larger values, for instance, the cap of 4 resulted in introducing  
540 unrealistic shifts to histogram of half-hourly precipitation rates for the month. Additionally, early in  
541 TRMM the lower bound of 0.5 was applied, which suggested a smaller value of the lower bound allows  
542 matching between the two accumulations without creating the egregious high snapshot values when the  
543 upper bound was expanded too far.

544 Inspired by the range of the ratio values between the monthly satellite-gauge and the monthly  
545 accumulation of half-hourly multi-satellite-only fields in generating IMERG, we consider the range [0,  
546 1.5] of the daily spatial disaggregation weights in this study is reasonable after careful checking the  
547 distributions of the spatial disaggregation weights. The lower bound of 0 was selected based on the  
548 consideration if the IMERG did not capture the daily precipitation event, then the spatial disaggregation  
549 weight is still equal to zero, which agrees as most as possible to the original IMERG. While there are at  
550 least two reasons for setting the upper bound of the spatial disaggregation weights as 1.5: (1) most  
551 numerical values of spatial disaggregation weights are in the range [0, 1.5], and (2) there are obvious  
552 anomalies in the final calibrated AIMERG, especially along the coastal regions and edges of the specific  
553 precipitation event coverages, where the values of the spatial disaggregation weights are larger than 1.5.  
554 Though the range [0, 1.5] of spatial disaggregation weights was applied to obtain the final AIMERG in  
555 this study, we also consider that this is still an open-ended question issue.

### 556 **5.3. The advantages of APHRODITE data in anchoring the multi-satellite-only precipitation** 557 **product**

558 It has been a great challenge to obtain precipitation estimates over the Tibetan Plateau and its  
559 surroundings, as there are very limited ground observations in this region, especially in its western parts  
560 (Ma et al., 2017). Incorporating a uniform precipitation gauge analysis is important and critical for  
561 controlling the bias that typifies the satellite precipitation estimates, e.g., using GPCC for TMPA and

562 IMERG (Huffman et al., 2019a). Those projects (e.g., GPCC, TRMM, GPM) demonstrate that even  
563 monthly gauge analyses contribute significant improvements on the satellite-only precipitation estimates,  
564 at least for some regions in some seasons. Primarily explorations at CPC suggested substantial  
565 improvements in the bias corrections using daily gauge analysis, especially for regions, where there is a  
566 dense network of gauges (Mega et al., 2014). Foreseeably, GPM would try their best to calibrate the GPM  
567 multi-~~satellite~~-satellite-only precipitation estimates at finer spatio-temporal scales (e.g., 0.25°/daily)  
568 worldwide.

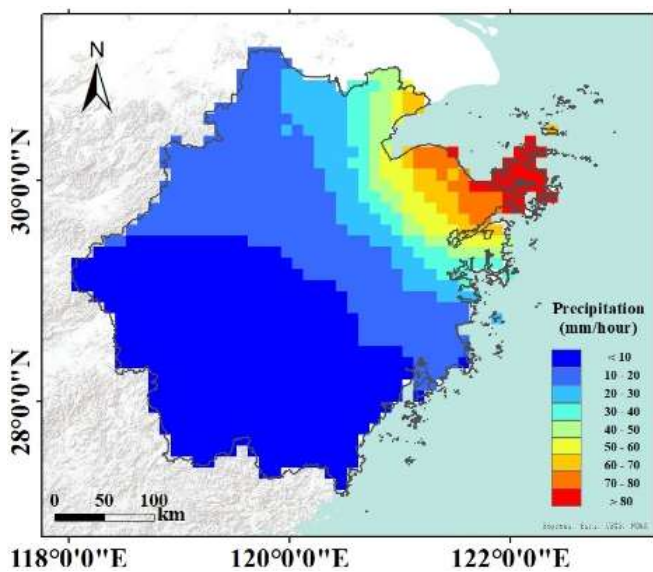
569 Currently, GPCC has been adopted to calibrate the TRMM TMPA and GPM IMERG at monthly  
570 scale. The Deutscher Wetterdienst (DWD) Global Precipitation Climatology Centre (GPCC) was  
571 established in 1989 to provide high-quality precipitation analyses over land based on conventional  
572 precipitation gauges from ~7,000-8,000 stations world-wide (Schneider et al. 2014, 2018). And two  
573 GPCC products were applied in the IMERG, the V8 Full Data Analysis for the majority of the time  
574 (currently 1998-2016), and the V6 Monitoring Product from 2017 to the then-present. Compared with  
575 GPCC, APHRODITE has inherently advantages with significantly larger numbers of ground observations  
576 and finer spatio-temporal resolutions, over the Asia. APHRODITE projects aimed at collecting as most  
577 gauge information as possible from the Asian countries. There are mainly three kinds of gauge  
578 information sources used in APHRODITE analysis, the GTS-based data, data precompiled by other  
579 projects or organizations, and APHRODITE's own collection. More detailed information on the  
580 APHRODITE' data sources could be found at the website (<http://www.chikyu.ac.jp/precip/>) and the

581 research of Yatagai (2012). Compared with the GPCC with the limited ground observations in and around  
582 the Tibetan Plateau in China, the neighboring countries provide plenty of ground observations in the  
583 APHRODITE data, in mountainous regions, and semi-arid and arid regions. Additionally, the spatio-  
584 temporal resolutions of APHRODITE ( $0.25^\circ$ /daily) are finer than those of GPCC ( $1.0^\circ$ /monthly).  
585 Therefore, APHRODITE has significant advantages in calibrating the IMERG data at daily scale.

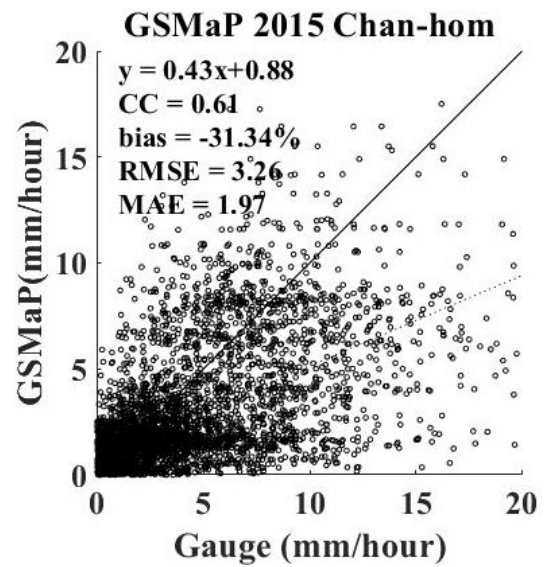
#### 586 ~~5.4. Quantitatively and horizontally comparisons with other high resolution precipitation product~~

587 ~~Recently, Tang et al (2020) has conducted a comprehensive comparison of GPM IMERG with~~  
588 ~~other nine state-of-the-art high resolution precipitation products, six satellite-based precipitation products~~  
589 ~~(TRMM 3B42,  $0.25^\circ/3$  hour; CMORPH,  $0.25^\circ/3$  hour; PERSIANN-CDR,  $0.25^\circ/1$  day; GSMaP  $0.1^\circ/1$~~   
590 ~~hour; CHIRPS,  $0.05^\circ/1$  day; SM2RAIN,  $0.25^\circ/1$  day) and three reanalysis datasets (ERA5,  $0.25^\circ/1$  hour;~~  
591 ~~ERA-Interim,  $0.75^\circ/3$  hour; MERRA2  $0.5^\circ \times 0.625^\circ/1$  hour) from 2000 to 2018, and found that the~~  
592 ~~IMERG product generally outperformed other datasets, except the Global Satellite Mapping of~~  
593 ~~Precipitation (GSMaP), which was adjusted at the daily scale by the gauge analysis ( $0.5^\circ$ /daily) from the~~  
594 ~~CPC (Mega et al., 2014). Therefore, we have compared the AIMERG with GSMaP, in case of the typhoon~~  
595 ~~Chan-hom, which is coordinated with those in Figure 11. As shown in Fig. 14, though the spatial patterns~~  
596 ~~of the GSMaP are similar with those of the AIMERG, the AIMERG provides much more details than~~  
597 ~~GSMaP, especially over the northeastern Zhejiang Province. Meanwhile, AIMERG significantly~~  
598 ~~overwhelms GSMaP in terms of both bias and random errors. For instance, GSMaP underestimates the~~

599 precipitation (bias  $\sim$  31%) twice as large as AIMERG (bias  $\sim$  15%), and the random errors of GSMaP  
 600 (MAE  $\sim$  1.97 mm/hour, RMSE  $\sim$  3.26 mm/hour) are also significantly larger than those of AIMERG  
 601 (MAE  $\sim$  1.44 mm/hour, RMSE  $\sim$  2.50 mm/hour). Compared with the original IMERG in Figure 11,  
 602 though the random errors of GSMaP are relatively larger, the bias of GSMaP ( $\sim$  31%) is significantly  
 603 smaller than that of the original IMERG ( $\sim$  50%), which owes to the calibrations on the GSMaP at the  
 604 daily scale. In future, we also encourage researchers to comprehensively evaluate and compare the  
 605 AIMERG with other high resolution precipitation products at various spatio-temporal scales.



(a)



(b)

606 Figure 14. The typhoon, Chan-hom, is selected as an example for assessing the quality of the Gauge  
 607 adjusted GSMaP, occurred in the typical period 0 a.m.,—11 a.m., July, 11, 2015, in Zhejiang Province,  
 608 which is coordinated with those in Figure 11. The background map used in this study was provided by

609 Esri, USGS and NOAA ([http://gato.arcgisonline.com/maps/World\\_Terrain\\_Base](http://gato.arcgisonline.com/maps/World_Terrain_Base), last access: 17 January  
610 2020).

~~611 The extent of the AIMERG could cover the Northern Eurasia, Middle East, Monsoon Asia, and  
612 Japan. This study mainly evaluated the AIMERG in the China Mainland, which calls for Asia wide  
613 evaluations in the future to assess both the algorithm and the corresponding precipitation product.~~

## 614 6. Data Availability

615 The AIMERG data record (0.1°/half-hourly, 2000-2015, Asia) is freely available at [http://argi-  
616 basic.hihanlin.com:8000/d/d925fecf60/](http://argi-basic.hihanlin.com:8000/d/d925fecf60/). Additionally, the AIMERG data is also freely accessible at  
617 <https://doi.org/10.5281/zenodo.3609352> (for the period from 2000 to 2008) (Ma et al., 2020a) and  
618 <http://doi.org/10.5281/zenodo.3609507> (for the period from 2009 to 2015) (Ma et al., 2020b).

## 620 7. Conclusions

621 As the milestone in the satellite-based precipitation measurement process, the TRMM and its  
622 successor GPM generate the most popular and the state-of-the-art satellite precipitation products for both  
623 water cycle related scientific researches and applications, TMPA (1998-present, 0.25°/3 hourly) and  
624 IMERG (2014-present, 0.1°/half-hourly), as well as the retrospective IMERG (2000-present, 0.1°/half-  
625 hourly) from GPM era to TRMM era. In this study, focusing on the potential drawbacks in generating

626 IMERG and its recently updated retrospective IMERG (finished in July, 2019), which were only  
627 calibrated at monthly scale using limited ground observations, GPCC (1.0°/monthly), resulting the  
628 IMERG with large systematic bias and random errors, we introduce another daily gauge analysis product,  
629 APHRODITE (Last update October 5, 2018), to calibrate the IMERG at 0.25°/daily scale. Compared with  
630 GPCC, APHRODITE has inherently advantages with significantly larger numbers of ground observations  
631 and finer spatio-temporal resolutions (0.25°/daily), over the Asia.

632 We have proposed a new algorithm (Daily Spatio-Temporal Disaggregation Calibration Algorithm,  
633 DSTDCA) for calibrating IMERG at daily scale, and provided a new AIMERG precipitation dataset  
634 (0.1°/half-hourly, 2000-2015, Asia) (Ma et al., 2020a, b) with better quality, calibrated by APHRODITE  
635 at daily scale for the Asian applications. And the main conclusions include but not limited to: (1) the  
636 proposed daily calibration algorithm is effective in considering the advantages from both satellite-based  
637 precipitation estimates and the ground observations; (2) AIMERG performs better than IMERG at  
638 different spatio-temporal scales, in terms of both systematic biases and random errors, over the China  
639 Main land; and (3) APHRODITE demonstrates significant advantages than GPCC in calibrating the  
640 IMERG, especially over the mountainous regions with complex terrain, e.g., the Tibetan Plateau.  
641 Additionally, results of this study suggests that it is a promising and applicable daily calibration algorithm  
642 for GPM in generating the future IMERG in either operational scheme or retrospective manner.

643

644 **Author Contributions**

645 Dr. Ziqiang Ma designed and organized the manuscript. Drs. Jintao Xu, Siyu Zhu, Jun Yang and  
646 Yuanjian Yang prepared the related materials and run the models for generating AIMERG and the related  
647 assessments. Dr. Guoqiang Tang and Prof. Zhou Shi made contributions on the scientific framework of  
648 this study and discussed the interpretation of results. Prof. Yang Hong co-advised this study. All authors  
649 discussed the results and commented on the manuscript.

650

651 **Competing interests**

652 The authors declare they have no competing financial interests.

653 **Acknowledgments**

654 This study was financially supported by the Key R&D Program of Ministry of Science and  
655 Technology, China (Grant No. 2018YFC1506500); the National Natural Science Foundation of China  
656 (Grant No. 41901343); The Second Tibetan Plateau Scientific Expedition and Research (STEP) program  
657 (grant no. 2019QZKK0105); the China Postdoctoral Science Foundation (No. 2018M630037, and  
658 2019T120021); the National Natural Science Foundation of China (Grant No. 91437214); the Open Fund  
659 of the State Key Laboratory of Remote Sensing Science, China (Grant No. OFSLRSS201909), the State  
660 Key Laboratory of Resources and Environmental Information System, China.



661 The contribution of the data providers is also greatly appreciated, including the Chinese  
662 Meteorological Data Sharing Service System (<http://cdc.nmic.cn/home.do>), the APHRODITE data  
663 provider (<http://aphrodite.st.hirosaki-u.ac.jp/download/>), and the IMERG data provider  
664 (<https://pmm.nasa.gov/data-access/downloads/gpm>).

665

666 **References**

- 667 Adler, R. F., Huffman, G. J., Chang, A., Ferraro, R., Xie, P., Janowiak, J., Rudolf, B., Schneider, U.,  
668 Curtis, S., Bolvin, D., Gruber, A., Susskind, J., Arkin, P., and Nelkin, E.: The Version-2 Global  
669 Precipitation Climatology Project (GPCP) Monthly Precipitation Analysis (1979–Present), *J.*  
670 *Hydrometeorol.*, 4, 1147–1167, [https://doi.org/10.1175/1525-](https://doi.org/10.1175/1525-7541(2003)004<1147:TVGPCP>2.0.CO;2)  
671 [7541\(2003\)004<1147:TVGPCP>2.0.CO;2](https://doi.org/10.1175/1525-7541(2003)004<1147:TVGPCP>2.0.CO;2), 2003.
- 672 Adler, R.F., Sapiano, M., Huffman, G.J., Wang, J.-J., Gu, G., Bolvin, D.T., Chiu, L., Schneider, U.,  
673 Becker, A., Nelkin, E.J., Xie, P., Ferraro, R., and Shin, D.-B.: The Global Precipitation Climatology  
674 Project (GPCP) Monthly Analysis (New Version 2.3) and a Review of 2017 Global  
675 Precipitation, *Atmos.*, 9(4), 138, <https://doi.org/10.3390/atmos9040138>, 2018.
- 676 Beck, H. E., van Dijk, A. I. J. M., Levizzani, V., Schellekens, J., Miralles, D. G., Martens, B., and Roo,  
677 A. d.: MSWEP: 3-hourly 0.25° global gridded precipitation (1979–2015) by merging gauge,  
678 satellite, and reanalysis data, *Hydrol. Earth Syst. Sci.*, 21, 589-615, [https://doi.org/10.5194/hess-21-](https://doi.org/10.5194/hess-21-589-2017)  
679 [589-2017](https://doi.org/10.5194/hess-21-589-2017), 2017.
- 680 Beck, H. E., Wood, E. F., Pan, M., Fisher, C. K., Miralles, D. G., van Dijk, A. I. J. M., McVicar, T. R.,  
681 and Adler, R. F.: MSWEP V2 Global 3-Hourly 0.1° Precipitation: Methodology and Quantitative  
682 Assessment, *Bull. Amer. Meteorol. Soc.*, 100, 473-500, [https://doi.org/10.1175/BAMS-D-17-](https://doi.org/10.1175/BAMS-D-17-0138.1)  
683 [0138.1](https://doi.org/10.1175/BAMS-D-17-0138.1), 2018.

- 684 Chen, M., Xie, P., Janowiak, J., and Arkin, P.: Global Land Precipitation: A 50-yr Monthly Analysis  
685 Based on Gauge Observations, *J. Hydrometeorol.*, 3, 249-266, [https://doi.org/10.1175/1525-](https://doi.org/10.1175/1525-7541(2002)003<0249:GLPAYM>2.0.CO;2)  
686 [7541\(2002\)003<0249:GLPAYM>2.0.CO;2](https://doi.org/10.1175/1525-7541(2002)003<0249:GLPAYM>2.0.CO;2), 2002.
- 687 Duncan, J. M. A., and Biggs, E. M.: Assessing the accuracy and applied use of satellite-derived  
688 precipitation estimates over Nepal, *Appl. Geogr.*, 34, 626–638,  
689 <https://doi.org/10.1016/j.apgeog.2012.04.001>, 2014.
- 690 Ebert, E. E., Janowiak, J. E., and Kidd, C.: Comparison of Near-Real-Time Precipitation Estimates from  
691 Satellite Observations and Numerical Models, *Bull. Amer. Meteorol. Soc.*, 88, 47-64,  
692 <https://doi.org/10.1175/BAMS-88-1-47>, 2007.
- 693 Hamada, A., Arakawa, O., and Yatagai, A.: An automated quality control method for daily rain-gauge  
694 data, *Global Environmental Research*, 15, 183-192, [http://www.airies.or.jp/journal\\_15-2eng.html](http://www.airies.or.jp/journal_15-2eng.html),  
695 2011.
- 696 Hong, Y., Hsu, K.-L., Sorooshian, S., and Gao, X.: Precipitation Estimation from Remotely Sensed  
697 Imagery Using an Artificial Neural Network Cloud Classification System, *J. Appl. Meteorol.*, 43,  
698 1834-1853, <https://doi.org/10.1175/JAM2173.1>, 2004.
- 699 Huffman, G. J., Adler, R. F., Arkin, P., Chang, A., Ferraro, R., Gruber, A., Janowiak, J., McNab, A.,  
700 Rudolf, B., and Schneider, U.: The Global Precipitation Climatology Project (GPCP) Version 1 data

701 set, Bull. Am. Meteorol. Soc., 78, 5-20, <https://doi.org/10.1175/1520->  
702 0477(1997)078<0005:TGPCPG>2.0.CO;2, 1997.

703 Huffman, G. J., Bolvin, D. T., Nelkin, E. J., Wolff, D. B., Adler, R. F., Gu, G., Hong, Y., Bowman, K. P.,  
704 and Stocker, E. F.: The TRMM Multisatellite Precipitation Analysis (TMPA): Quasi-Global,  
705 Multiyear, Combined-Sensor Precipitation Estimates at Fine Scales, J. Hydrometeorol., 8, 38-55,  
706 <https://doi.org/10.1175/JHM560.1>, 2007.

707 Huffman, G. J., Bolvin, D. T., Braithwaite, D., Hsu, K., Joyce, R., Kidd, C., Nelkin, E. J., Sorooshian, S.,  
708 Tan, J., and Xie, P.: NASA Global Precipitation Measurement (GPM) Integrated Multi-satellitE  
709 Retrievals for GPM (IMERG), Algorithm Theoretical Basis Document (ATBD) Version 06,  
710 NASA/GSFC, Greenbelt, MD, USA, 38pp., 2019a.

711 Huffman, G. J., E.F. Stocker, D.T. Bolvin, E.J. Nelkin, and Jackson Tan: GPM IMERG Final  
712 Precipitation L3 Half Hourly 0.1 degree x 0.1 degree V06, Greenbelt, MD, Goddard Earth Sciences  
713 Data and Information Services Center (GES DISC), <https://doi.org/10.5067/GPM/IMERG/3B->  
714 HH/06, 2019b.

715 Joyce, R. J., Janowiak, J. E., Arkin, P. A., and Xie, P.: CMORPH: A Method that Produces Global  
716 Precipitation Estimates from Passive Microwave and Infrared Data at High Spatial and Temporal  
717 Resolution, J. Hydrometeorol., 5, 487-503, <https://doi.org/10.1175/1525->  
718 7541(2004)005<0487:CAMTPG>2.0.CO;2, 2004.

- 719 Lu, H., Ding, L., Ma, Z., Li, H., Lu, T., Su, M., and Xu, J.: Spatiotemporal Assessments on the Satellite-  
720 Based Precipitation Products From Fengyun and GPM Over the Yunnan-Kweichow Plateau, China,  
721 Earth Space Sci., 7, e2019EA000857, <https://doi.org/10.1029/2019EA000857>, 2020.
- 722 Mega, T., Ushio, T., Kubota, T., Kachi, M., Aonashi, K., and Shige, S.: Gauge adjusted global satellite  
723 mapping of precipitation (GSMaP\_Gauge), in: 2014 XXXIth URSI General Assembly and  
724 Scientific Symposium (URSI GASS), Beijing, China, 17-23 August 2014,1–4. 2014.
- 725 Ménégoz, M., Gallée, H., and Jacobi, H. W.: Precipitation and snow cover in the Himalaya: from  
726 reanalysis to regional climate simulations, Hydrol. Earth Syst. Sci., 17, 3921–3936,  
727 <https://doi.org/10.5194/hess-17-3921-2013>, 2013.
- 728 Ma, Z., Jin, X., Zhu, S., Tang, G., Yang, Y., Shi, Z., and Hong, Y.: AIMERG: a new Asian precipitation  
729 dataset (0.1°/half-hourly, 2000-2008) by calibrating GPM IMERG at daily scale using  
730 APHRODITE [Data set], Zenodo, <https://doi.org/10.5281/zenodo.3609352>, 2020.
- 731 Ma, Z., Jin, X., Zhu, S., Tang, G., Yang, Y., Shi, Z., and Hong, Y.: AIMERG: a new Asian precipitation  
732 dataset (0.1°/half-hourly, 2009-2015) by calibrating GPM IMERG at daily scale using  
733 APHRODITE [Data set], Zenodo, <https://doi.org/10.5281/zenodo.3609507>, 2020.
- 734 Ma, Z., Shi, Z., Zhou, Y., Xu, J., Yu, W., and Yang, Y.: A spatial data mining algorithm for downscaling  
735 TMPA 3B43 V7 data over the Qinghai–Tibet Plateau with the effects of systematic anomalies  
736 removed, Remote Sens. Environ., 200, 378-395, <https://doi.org/10.1016/j.rse.2017.08.023>, 2017.

- 737 [Ma, Z., Tan, X., Yang, Y., Chen, X., Kan, G., Ji, X., Lu, H., Long, J., Cui, Y., and Hong, Y.: The First](#)  
738 [Comparisons of IMERG and the Downscaled Results Based on IMERG in Hydrological Utility](#)  
739 [over the Ganjiang River Basin, Water-sui, 10\(10\), 1392, <https://doi.org/10.3390/w10101392>, 2018.](#)
- 740 Matsuura, K., and Willmott C. J.: Terrestrial precipitation: 1900–2008 gridded monthly time series  
741 (version 2.01), Center for Climatic Research Department of Geography Center for Climatic  
742 Research, University of Delaware,  
743 [http://climate.geog.udel.edu/~climate/html\\_pages/Global2\\_Ts\\_2009/README.global\\_p\\_ts\\_200](http://climate.geog.udel.edu/~climate/html_pages/Global2_Ts_2009/README.global_p_ts_2009.html)  
744 [9.html](http://climate.geog.udel.edu/~climate/html_pages/Global2_Ts_2009/README.global_p_ts_2009.html), 2009.
- 745 Mitchell, T. D., and Jones, P. D.: An improved method of constructing a database of monthly climate  
746 observations and associated high-resolution grids, *Int. J. Climatol.*, 25, 693-712,  
747 <https://doi.org/10.1002/joc.1181>, 2005.
- 748 Rajeevan, M., and Bhate, J.: A high resolution daily gridded rainfall dataset (1971–2005) for mesoscale  
749 meteorological studies, *Curr. Sci.*, 96, 558-562, <https://www.jstor.org/stable/24105470>, 2009.
- 750 Rozante, J. R., Moreira, D. S., Goncalves, L.G., and Vila, D. A.: Combining TRMM and surface  
751 observations of precipitation: technique and validation over South America, *Wea. Forecasting*, 25,  
752 885-894, <https://doi.org/10.1175/2010WAF2222325.1>, 2010.
- 753 Schneider, U., Fuchs, T., Meyer-Christoffer, A., and Rudolf, B.: Global precipitation analysis  
754 products of the GPCC. Global Precipitation Climatology Centre, DWD, 13 pp., 2008
- 755 Schneider, U., Becker, A., Finger, P., Meyer-Christoffer, A., Ziese, M., and Rudolf, B.: GPCC's new land

756 surface precipitation climatology based on quality-controlled in situ data and its role in  
757 quantifying the global water cycle, *Theor. Appl. Climatol.*, 115, 15-40,  
758 <https://doi.org/10.1007/s00704-013-0860-x>, 2014.

759 Schneider, U., P. Finger, A. Meyer-Christoffer, M. Ziese, A. Becker: Global Precipitation Analysis  
760 Products of the GPCP. GPCP Internet Publication, DWD, 17 pp., 2018

761 Shen, Y., Feng, M. N. Zhang, H. Z. and Gao, X.: Interpolation methods of China daily precipitation data  
762 [in Chinese], *J. Appl. Meteorol. Sci.*, 21, 279–286, <https://doi.org/10.11898/1001-7313.20100303>,  
763 2010.

764 Shen, Y., Zhao, P., Pan, Y., and Yu, J.: A high spatiotemporal gauge-satellite merged precipitation analysis  
765 over China, *J. Geophys. Res. Atmos.*, 119, <https://doi.org/10.1002/2013JD020686>, 2014.

766 Sorooshian, S., Hsu, K.-L., Gao, X., Gupta, H. V., Imam, B., and Braithwaite, D.: Evaluation of  
767 PERSIANN System Satellite-Based Estimates of Tropical Rainfall, *Bull. Amer. Meteorol. Soc.*,  
768 81, 2035-2046, [https://doi.org/10.1175/1520-0477\(2000\)081<2035:EOPSSE>2.3.CO;2](https://doi.org/10.1175/1520-0477(2000)081<2035:EOPSSE>2.3.CO;2), 2000.

769 Sunilkumar, K., Yatagai, A., and Masuda, M.: Preliminary evaluation of GPM-IMERG rainfall estimates  
770 over three distinct climate zones with APHRODITE. *Earth Space Sci.*, 6, 1321– 1335.  
771 <https://doi.org/10.1029/2018EA000503>, 2019.

772 Tang, G., Ma, Y., Long, D., Zhong, L., and Hong, Y.: Evaluation of GPM Day-1 IMERG and TMPA  
773 Version-7 legacy products over Mainland China at multiple spatiotemporal scales, *J. Hydrol.*, 533,  
774 152-167, <https://doi.org/10.1016/j.jhydrol.2015.12.008>, 2016.

775 Tang, G., Clark, M. P., Papalexiou, S. M., Ma, Z., and Hong, Y.: Have satellite precipitation products  
776 improved over last two decades? A comprehensive comparison of GPM IMERG with nine satellite  
777 and reanalysis datasets, *Remote Sens. Environ.*, 240, 111697,  
778 <https://doi.org/10.1016/j.rse.2020.111697>, 2020.

779 Xie, P., and Xiong, A.: A conceptual model for constructing high-resolution gauge-satellite merged  
780 precipitation analyses, *J. Geophys. Res. Atmos.*, 116, <https://doi.org/10.1029/2011JD016118>,  
781 2011.

782 Xu, J., Ma, Z., Tang, G., Ji, Q., Min, X., Wan, W., and Shi, Z.: Quantitative Evaluations and Error Source  
783 Analysis of Fengyun-2-Based and GPM-Based Precipitation Products over Mainland China in  
784 Summer, 2018, *Remote Sens.*, 11, <https://doi.org/10.3390/rs11242992>, 2019.

785 Yatagai, A., Xie, P., and Kitoh, A.: Utilization of a New Gauge-based Daily Precipitation Dataset over  
786 Monsoon Asia for Validation of the Daily Precipitation Climatology Simulated by the MRI/JMA  
787 20-km-mesh AGCM, *SOLA*, 1, 193-196, <https://doi.org/10.2151/sola.2005-050>, 2005.

788 Yatagai, A., Kamiguchi, K., Arakawa, O., Hamada, A., Yasutomi, N., and Kitoh, A.: APHRODITE:  
789 Constructing a Long-Term Daily Gridded Precipitation Dataset for Asia Based on a Dense Network  
790 of Rain Gauges, *Bull. Amer. Meteorol. Soc.*, 93, 1401-1415, [https://doi.org/10.1175/BAMS-D-11-](https://doi.org/10.1175/BAMS-D-11-00122.1)  
791 00122.1, 2012.



792 Yong, B., Ren, L.-L., Hong, Y., Wang, J.-H., Gourley, J. J., Jiang, S.-H., Chen, X., and Wang, W.:  
793 Hydrologic evaluation of Multisatellite Precipitation Analysis standard precipitation products in  
794 basins beyond its inclined latitude band: A case study in Laohahe basin, China, *Water Resour. Res.*,  
795 46, <https://doi.org/10.1029/2009WR008965>, 2010.

796

797

798

799 **Appendix A: Acronyms with definitions used in this study.**

AIMERG	Asian precipitation dataset by calibrating GPM IMERG at daily scale using APHRODITE
APHRODITE	Asian Precipitation Highly Resolved Observational Data Integration Towards Evaluation of Water Resources
ATBD	Algorithm Theoretical Basis Document
BIAS	Relative Bias
CC	Correlation Coefficient
CHIRPS	Climate Hazards group Infrared Precipitation with Stations
CLIMAT	Monthly Climatological Data
CMA	Chinese Meteorological Administration
CMORPH	Climate Prediction Center (CPC) MORPHing technique
CPC	Climate Prediction Center
CSI	Critical Success Index
DSTDCA	Daily Spatio-Temporal Disaggregation Calibration Algorithm
DWD	Deutscher Wetterdienst
ERA5	Fifth generation of ECMWF atmospheric reanalyses of the global climate
ERA-Interim	ECMWF ReAnalysis Interim
FAR	False Alarm Ratio
GEWEX	Global Energy and Water Exchange
GPCC	Global Precipitation Climatology Centre

GPM	Global Precipitation Measurement
GSMaP	Gauge-adjusted Global Satellite Mapping of Precipitation V7
GTS	Global Telecommunications System
IMERG	Integrated Multi-satellitE Retrievals for GPM
IR	Infrared
MAE	Mean <u>Absolute</u> Error
MERRA2	The Modern-Era Retrospective Analysis for Research and Applications, Version 2
MW	Microwave
NHMs	National hydrological and meteorological services
NMIC	National Meteorological Information Center
OI	Optimal Interpolation
PDF	Probability Density Function
PERSIANN	Precipitation Estimation from Remotely Sensed Information using Artificial Neural Networks
PERSIANN-CCS	Precipitation Estimation from Remotely Sensed Information using Artificial Neural Networks-Cloud Classification System
PERSIANN-CDR	PERSIANN-Climate Data Record
PMW	Passive Microwave
POD	Probability of Detection

QC	Quality Control
RMSD	Root- <del>m</del> <u>M</u> ean- <del>S</del> <u>S</u> quare Deviation
RMSE	Root Mean Square Error
SG	Satellite-Gauge
SM2RAIN	Soil Moisture to RAIN based on ESA Climate Change Initiative (CCI)
SYNOP	Synoptic Weather Report
TMPA	TRMM Multi-satellite Precipitation Analysis
TRMM 3B42	Tropical Rainfall Measuring Mission Multi-satellite Precipitation Analysis 3B42 V7